CHAPTER

Environmental Characteristics

2

The sun is a sphere of intensely hot gaseous matter with a diameter of 1.39×10^9 m (see Figure 2.1). The sun is about 1.5×10^8 km away from earth, so, because thermal radiation travels with the speed of light in vacuum (about 300,000 km/s), after leaving the sun solar energy reaches our planet in 8 min and 20 s. As observed from the earth, the sun disk forms an angle of 32 min of a degree. This is important in many applications, especially in concentrator optics, where the sun cannot be considered as a point source and even this small angle is significant in the analysis of the optical behavior of the collector. The sun has an effective blackbody temperature of 5760 K. The temperature in the central region is much higher. In effect, the sun is a continuous fusion reactor in which hydrogen is turned into helium. The sun's total energy output is 3.8×10^{20} MW, which is equal to 63 MW/m^2 of the sun's surface. This energy radiates outward in all directions. The earth receives only a tiny fraction of the total radiation emitted, equal to 1.7×10^{14} kW; however, even with this small fraction, it is estimated that 84 min of solar radiation falling on earth is equal to the world energy demand for 1 year (about 900 EJ). As seen from the earth, the sun rotates around its axis about once every 4 weeks.

As observed from earth, the path of the sun across the sky varies throughout the year. The shape described by the sun's position, considered at the same time each day for a complete year, is called the *analemma* and resembles a figure 8 aligned along a north–south axis. The most obvious variation in the sun's apparent position through the year is a north–south swing over 47° of angle (because of the 23.5° tilt of the earth axis with respect to the sun), called *declination* (see Section 2.2). The north–south swing in apparent angle is the main cause for the existence of seasons on earth.

Knowledge of the sun's path through the sky is necessary to calculate the solar radiation falling on a surface, the solar heat gain, the proper orientation of solar collectors, the placement of collectors to avoid shading, and many more factors that are not of direct interest in this book. The objective of this

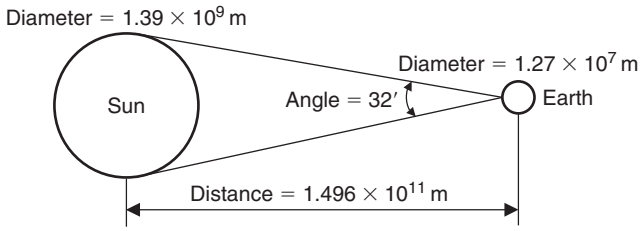

FIGURE 2.1

Sun–earth relationship.

Solar Energy Engineering. http://dx.doi.org/10.1016/B978-0-12-397270-5.00002-9
Copyright © 2014 Elsevier Inc. All rights reserved.

chapter was to describe the movements of the sun relative to the earth that give to the sun its east–west trajectory across the sky. The variation of solar incidence angle and the amount of solar energy received are analyzed for a number of fixed and tracking surfaces. The environment in which a solar system works depends mostly on the solar energy availability. Therefore, this is analyzed in some detail. The general weather of a location is required in many energy calculations. This is usually presented as a typical meteorological year (TMY) file, which is described in the last section of this chapter.

2.1 Reckoning of time

In solar energy calculations, apparent solar time (AST) must be used to express the time of day. AST is based on the apparent angular motion of the sun across the sky. The time when the sun crosses the meridian of the observer is the local solar noon. It usually does not coincide with the 12:00 o'clock time of a locality. To convert the local standard time (LST) to AST, two corrections are applied; the equation of time (ET) and longitude correction. These are analyzed next.

2.1.1 Equation of time

Due to factors associated with the earth's orbit around the sun, the earth's orbital velocity varies throughout the year, so the AST varies slightly from the mean time kept by a clock running at a uniform rate. The variation is called the *equation of time* (ET). The ET arises because the length of a day, that is, the time required by the earth to complete one revolution about its own axis with respect to the sun, is not uniform throughout the year. Over the year, the average length of a day is 24 h; however, the length of a day varies due to the eccentricity of the earth's orbit and the tilt of the earth's axis from the normal plane of its orbit. Due to the ellipticity of the orbit, the earth is closer to the sun on January 3 and furthest from the sun on July 4. Therefore the earth's orbiting speed is faster than its average speed for half the year (from about October through March) and slower than its average speed for the remaining half of the year (from about April through September).

The values of the ET as a function of the day of the year (N) can be obtained approximately from the following equations:

$$\mathrm{ET} = 9.87\sin(2B) - 7.53\cos(B) - 1.5\sin(B)\ [\mathrm{min}] \tag{2.1}$$

and

$$B = (N - 81)\frac{360}{364} \tag{2.2}$$

A graphical representation of Eq (2.1) is shown in Figure 2.2, from which the ET can be obtained directly.

2.1.2 Longitude correction

The standard clock time is reckoned from a selected meridian near the center of a time zone or from the standard meridian, the Greenwich, which is at longitude of 0°. Since the sun takes 4 min to transverse

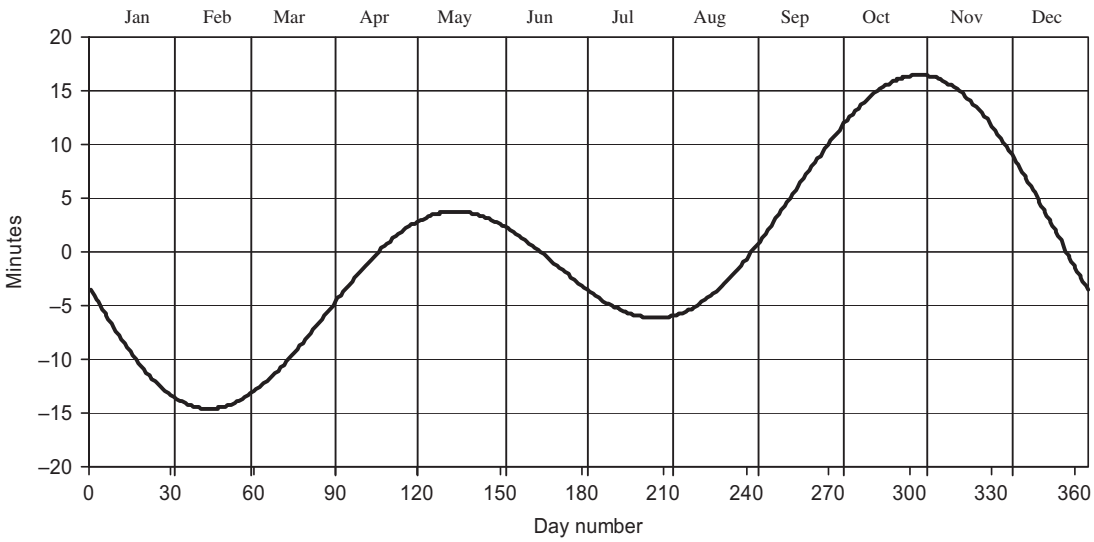

FIGURE 2.2

Equation of time.

1° of longitude, a longitude correction term of 4× (Standard longitude [SL] − Local longitude [LL]) should be either added or subtracted to the standard clock time of the locality. This correction is constant for a particular longitude, and the following rule must be followed with respect to sign convention. If the location is east of the standard meridian, the correction is added to the clock time. If the location is west, it is subtracted. The general equation for calculating the AST is:

$$\mathrm{AST} = \mathrm{LST} + \mathrm{ET} \pm 4(\mathrm{SL} - \mathrm{LL}) - \mathrm{DS} \tag{2.3}$$

where

LST = local standard time.
ET = equation of time.
SL = standard longitude.
LL = local longitude.
DS = daylight saving (it is either 0 or 60 min).

If a location is east of Greenwich, the sign of Eq (2.3) is minus (−), and if it is west, the sign is plus (+). If a daylight saving time is used, this must be subtracted from the LST. The term DS depends on whether daylight saving time is in operation (usually from end of March to end of October) or not. This term is usually ignored from this equation and considered only if the estimation is within the DS period.

EXAMPLE 2.1

Find the equation of AST for the city of Nicosia, Cyprus.

Solution

For the locality of Cyprus, the SL is 30°E. The city of Nicosia is at a LL of 33.33° east of Greenwich. Therefore, the longitude correction is $-4 \times (30-33.33) = +13.32$ min. Thus, Eq (2.3) can be written as:

$$\text{AST} = \text{LST} + \text{ET} + 13.32 \text{ (min)}$$

2.2 Solar angles

The earth makes one rotation about its axis every 24 h and completes a revolution about the sun in a period of approximately 365.25 days. This revolution is not circular but follows an ellipse with the sun at one of the foci, as shown in Figure 2.3. The eccentricity, e, of the earth's orbit is very small, equal to 0.01673. Therefore, the orbit of the earth round the sun is almost circular. The sun–earth distance, R, at perihelion (shortest distance, at January 3) and aphelion (longest distance, at July 4) is given by Garg (1982):

$$R = a(1 \pm e) \tag{2.4}$$

where a = mean sun–earth distance = 149.5985×10^6 km.

The plus sign in Eq (2.4) is for the sun–earth distance when the earth is at the aphelion position and the minus sign for the perihelion position. The solution of Eq (2.4) gives values for the longest distance

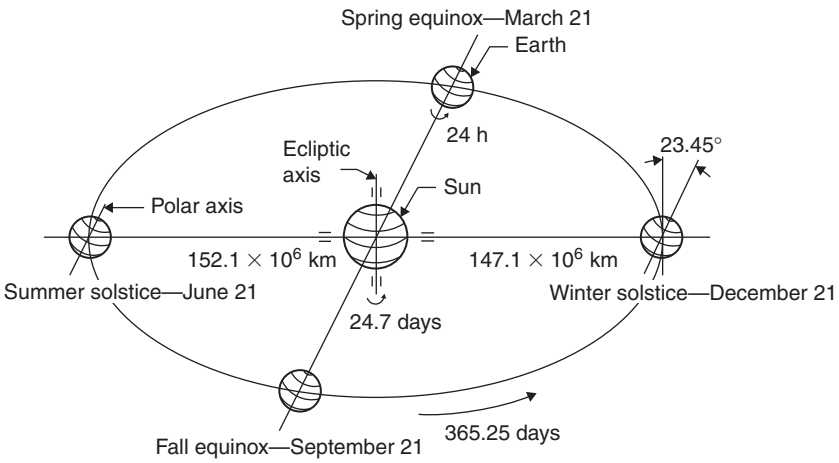

FIGURE 2.3

Annual motion of the earth about the sun.

equal to 152.1×10^6 km and for the shortest distance equal to 147.1×10^6 km, as shown in Figure 2.3. The difference between the two distances is only 3.3%. The mean sun–earth distance, a, is defined as half the sum of the perihelion and aphelion distances.

The sun's position in the sky changes from day to day and from hour to hour. It is common knowledge that the sun is higher in the sky in the summer than in winter. The relative motions of the sun and earth are not simple, but they are systematic and thus predictable. Once a year, the earth moves around the sun in an orbit that is elliptical in shape. As the earth makes its yearly revolution around the sun, it rotates every 24 h about its axis, which is tilted at an angle of 23° 27.14 min (23.45°) to the plane of the elliptic, which contains the earth's orbital plane and the sun's equator, as shown in Figure 2.3.

The most obvious apparent motion of the sun is that it moves daily in an arc across the sky, reaching its highest point at midday. As winter becomes spring and then summer, the sunrise and sunset points move gradually northward along the horizon. In the Northern Hemisphere, the days get longer as the sun rises earlier and sets later each day and the sun's path gets higher in the sky. On June 21 the sun is at its most northerly position with respect to the earth. This is called the *summer solstice* and during this day the daytime is at a maximum. Six months later, on December 21, the *winter solstice*, the reverse is true and the sun is at its most southerly position (see Figure 2.4). In the middle of the 6-month range, on March 21 and September 21, the length of the day is equal to the length of the night. These are called *spring* and *fall equinoxes*, respectively. The summer and winter solstices are the opposite in the Southern Hemisphere; that is, summer solstice is on December 21 and winter solstice is on June 21. It should be noted that all these dates are approximate and that there are small variations (difference of a few days) from year to year.

For the purposes of this book, the Ptolemaic view of the sun's motion is used in the analysis that follows, for simplicity; that is, since all motion is relative, it is convenient to consider the earth fixed and to describe the sun's virtual motion in a coordinate system fixed to the earth with its origin at the site of interest.

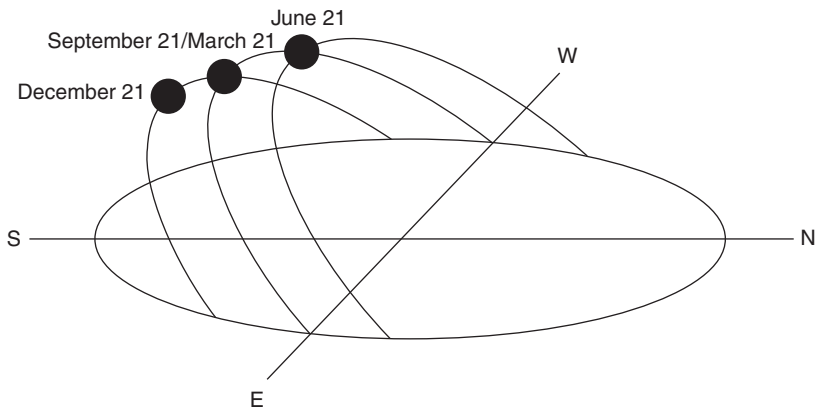

FIGURE 2.4

Annual changes in the sun's position in the sky (Northern Hemisphere).

For most solar energy applications, one needs reasonably accurate predictions of where the sun will be in the sky at a given time of day and year. In the Ptolemaic sense, the sun is constrained to move with 2 degrees of freedom on the celestial sphere; therefore, its position with respect to an observer on earth can be fully described by means of two astronomical angles, the solar altitude (α) and the solar azimuth (z). The following is a description of each angle, together with the associated formulation. An approximate method for calculating these angles is by means of sun path diagrams (see Section 2.2.2).

Before giving the equations of solar altitude and azimuth angles, the solar declination and hour angle need to be defined. These are required in all other solar angle formulations.

Declination, δ

As shown in Figure 2.3 the earth axis of rotation (the polar axis) is always inclined at an angle of 23.45° from the ecliptic axis, which is normal to the ecliptic plane. The ecliptic plane is the plane of orbit of the earth around the sun. As the earth rotates around the sun it is as if the polar axis is moving with respect to the sun. The solar declination is the angular distance of the sun's rays north (or south) of the equator, north declination designated as positive. As shown in Figure 2.5 it is the angle between the sun–earth centerline and the projection of this line on the equatorial plane. Declinations north of the equator (summer in the Northern Hemisphere) are positive, and those south are negative. Figure 2.6 shows the declination during the equinoxes and the solstices. As can be seen, the declination ranges from 0° at the spring equinox to +23.45° at the summer solstice, 0° at the fall equinox, and −23.45° at the winter solstice.

The variation of the solar declination throughout the year is shown in Figure 2.7. The declination, δ, in degrees for any day of the year (N) can be calculated approximately by the equation (ASHRAE, 2007):

$$\delta = 23.45 \sin\left[\frac{360}{365}(284 + N)\right] \tag{2.5}$$

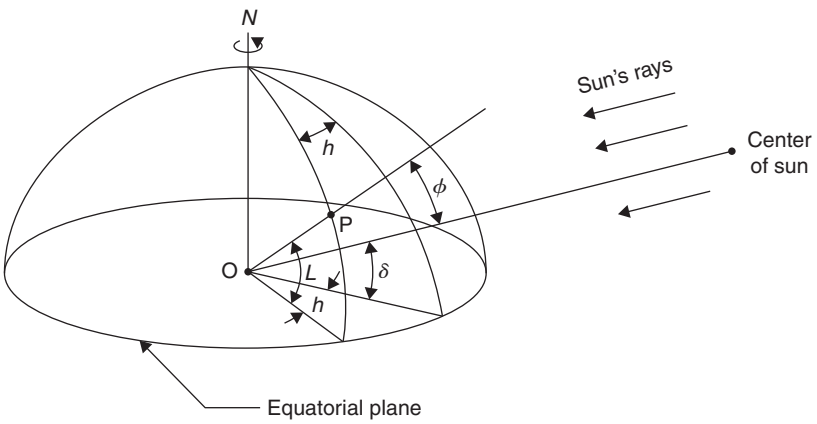

FIGURE 2.5

Definition of latitude, hour angle, and solar declination.

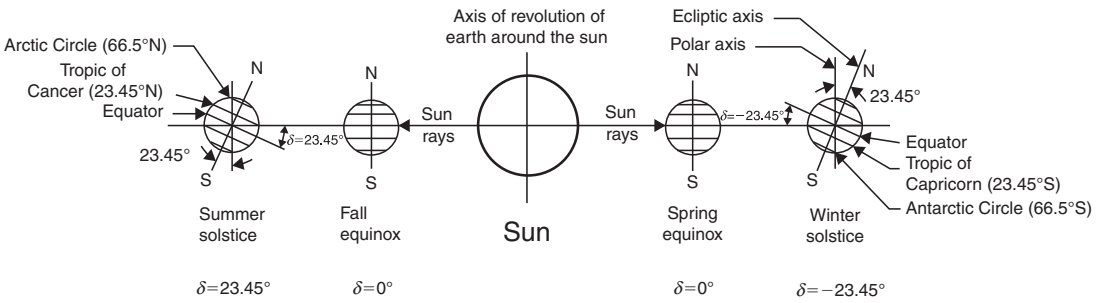

FIGURE 2.6

Yearly variation of solar declination.

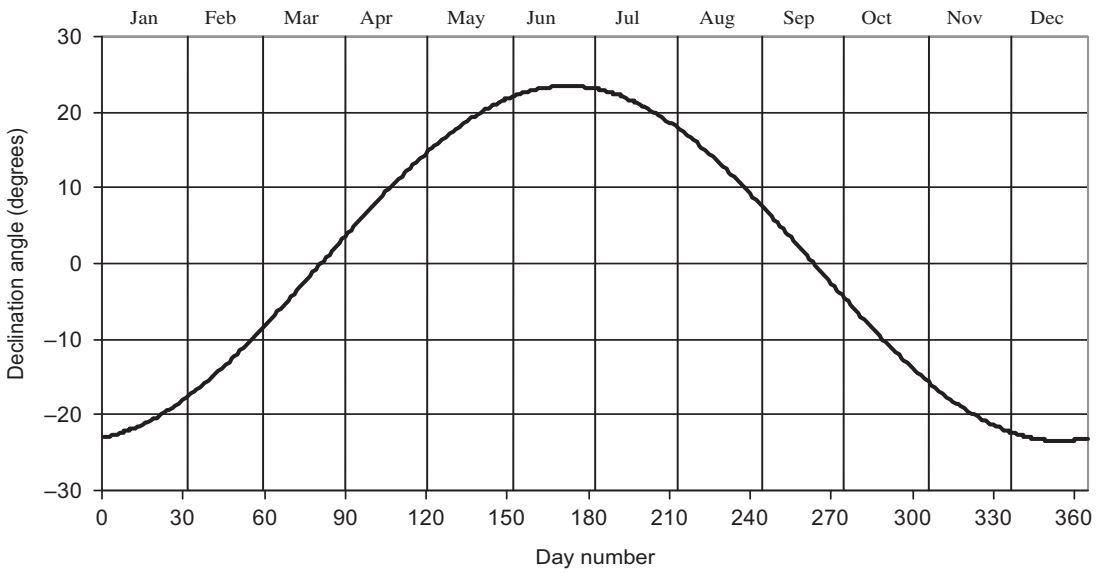

FIGURE 2.7

Declination of the sun.

Declination can also be given in radians[1] by the Spencer formula (Spencer, 1971):

$$\begin{aligned}\delta = {} & 0.006918 - 0.399912\cos(\Gamma) + 0.070257\sin(\Gamma) \\ & - 0.006758\cos(2\Gamma) + 0.000907\sin(2\Gamma) \\ & - 0.002697\cos(3\Gamma) + 0.00148\sin(3\Gamma)\end{aligned} \tag{2.6}$$

[1]Radians can be converted to degrees by multiplying by 180 and dividing by π.

Table 2.1 Day Number and Recommended Average Day for Each Month

Month	Day Number	Hour of the Month	Average Day of the Month		
			Date	*N*	δ (degrees)
January	i	k	17	17	−20.92
February	$31+i$	$744+k$	16	47	−12.95
March	$59+i$	$1416+k$	16	75	−2.42
April	$90+i$	$2160+k$	15	105	9.41
May	$120+i$	$2880+k$	15	135	18.79
June	$151+i$	$3624+k$	11	162	23.09
July	$181+i$	$4344+k$	17	198	21.18
August	$212+i$	$5088+k$	16	228	13.45
September	$243+i$	$5832+k$	15	258	2.22
October	$273+i$	$6552+k$	15	288	−9.60
November	$304+i$	$7296+k$	14	318	−18.91
December	$334+i$	$8016+k$	10	344	−23.05

where Γ is called the *day angle*, given (in radians) by:

$$\Gamma = \frac{2\pi(N-1)}{365} \tag{2.7}$$

The solar declination during any given day can be considered constant in engineering calculations (Kreith and Kreider, 1978; Duffie and Beckman, 1991).

As shown in Figure 2.6, the Tropics of Cancer (23.45°N) and Capricorn (23.45°S) are the latitudes where the sun is overhead during summer and winter solstices, respectively. Another two latitudes of interest are the Arctic (66.5°N) and Antarctic (66.5°S) Circles. As shown in Figure 2.6, at winter solstice all points north of the Arctic Circle are in complete darkness, whereas all points south of the Antarctic Circle receive continuous sunlight. The opposite is true for the summer solstice. During spring and fall equinoxes, the North and South Poles are equidistant from the sun and daytime is equal to nighttime, both of which equal 12 h.

Because the day number, the hour of the month, and the average day of each month are frequently required in solar geometry calculations, Table 2.1 is given for easy reference.

Hour angle, h

The hour angle, h, of a point on the earth's surface is defined as the angle through which the earth would turn to bring the meridian of the point directly under the sun. Figure 2.5 shows the hour angle of point P as the angle measured on the earth's equatorial plane between the projection of OP and the projection of the sun–earth center to center line. The hour angle at local solar noon is zero, with each 360/24 or 15° of longitude equivalent to 1 h, afternoon hours being designated as positive. Expressed symbolically, the hour angle in degrees is:

$$h = \pm 0.25\ (\text{Number of minutes from local solar noon}) \tag{2.8}$$

where the plus sign applies to afternoon hours and the minus sign to morning hours.

The hour angle can also be obtained from the AST; that is, the corrected local solar time:

$$h = (\text{AST} - 12)15 \tag{2.9}$$

At local solar noon, AST = 12 and $h = 0°$. Therefore, from Eq (2.3), the LST (the time shown by our clocks at local solar noon) is:

$$\text{LST} = 12 - \text{ET} \mp 4(\text{SL} - \text{LL}) \tag{2.10}$$

EXAMPLE 2.2

Find the equation for LST at local solar noon for Nicosia, Cyprus.

Solution

For the location of Nicosia, Cyprus, from Example 2.1,

$$\text{LST} = 12 - \text{ET} - 13.32 \text{ (min)}$$

EXAMPLE 2.3

Calculate the apparent solar time on March 10 at 2:30 pm for the city of Athens, Greece (23°40′E longitude).

Solution

The ET for March 10 ($N = 69$) is calculated from Eq (2.1), in which the factor B is obtained from Eq (2.2) as:

$$B = 360/364(N - 81) = 360/364(69 - 81) = -11.87$$

$$\begin{aligned}\text{ET} &= 9.87\sin(2B) - 7.53\cos(B) - 1.5\sin(B)\\ &= 9.87\sin(-2 \times 11.87) - 7.53\cos(-11.87) - 1.5\sin(-11.87)\end{aligned}$$

Therefore,

$$\text{ET} = -11.04 \text{ min} \sim -11 \text{ min}$$

The standard meridian for Athens is 30°E longitude. Therefore, the AST at 2:30 pm, from Eq (2.3), is:

$$\begin{aligned}\text{AST} &= 14{:}30 - 4(30 - 23.66) - 0{:}11 = 14{:}30 - 0{:}25 - 0{:}11\\ &= 13{:}54, \text{ or } 1{:}54 \text{ pm}\end{aligned}$$

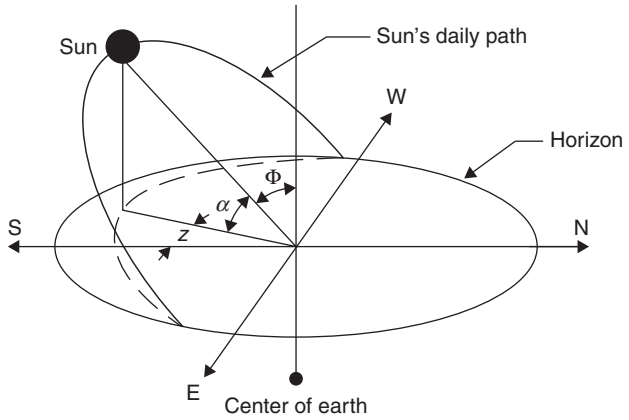

FIGURE 2.8

Apparent daily path of the sun across the sky from sunrise to sunset.

Solar altitude angle, α

The solar altitude angle is the angle between the sun's rays and a horizontal plane, as shown in Figure 2.8. It is related to the solar zenith angle, Φ, which is the angle between the sun's rays and the vertical. Therefore,

$$\Phi + \alpha = \pi/2 = 90^\circ \tag{2.11}$$

The mathematical expression for the solar altitude angle is:

$$\sin(\alpha) = \cos(\Phi) = \sin(L)\sin(\delta) + \cos(L)\cos(\delta)\cos(h) \tag{2.12}$$

where $L =$ local latitude, defined as the angle between a line from the center of the earth to the site of interest and the equatorial plane. Values north of the equator are positive and those south are negative.

Solar azimuth angle, z

The solar azimuth angle, z, is the angle of the sun's rays measured in the horizontal plane from due south (true south) for the Northern Hemisphere or due north for the Southern Hemisphere; westward is designated as positive. The mathematical expression for the solar azimuth angle is:

$$\sin(z) = \frac{\cos(\delta)\sin(h)}{\cos(\alpha)} \tag{2.13}$$

This equation is correct, provided that $\cos(h) > \tan(\delta)/\tan(L)$ (ASHRAE, 1975). If not, it means that the sun is behind the E–W line, as shown in Figure 2.4, and the azimuth angle for the morning hours is $-\pi + |z|$ and for the afternoon hours is $\pi - z$.

At solar noon, by definition, the sun is exactly on the meridian, which contains the north–south line, and consequently, the solar azimuth is 0°. Therefore the noon altitude α_n is:

$$\alpha_n = 90^\circ - L + \delta \tag{2.14}$$

EXAMPLE 2.4

What are the maximum and minimum noon altitude angles for a location at 40° latitude?

Solution

The maximum angle is at summer solstice, where δ is maximum, that is, 23.5°. Therefore, the maximum noon altitude angle is $90° - 40° + 23.5° = 73.5°$.

The minimum noon altitude angle is at winter solstice, where δ is minimum, that is, −23.5°. Therefore, the minimum noon altitude angle is $90° - 40° - 23.5° = 26.5°$.

Sunrise and sunset times and day length

The sun is said to rise and set when the solar altitude angle is 0. So, the hour angle at sunset, h_{ss}, can be found by solving Eq. (2.12) for h when $\alpha = 0°$:

$$\sin(\alpha) = \sin(0) = 0 = \sin(L)\sin(\delta) + \cos(L)\cos(\delta)\cos(h_{ss})$$

or

$$\cos(h_{ss}) = -\frac{\sin(L)\sin(\delta)}{\cos(L)\cos(\delta)}$$

which reduces to:

$$\cos(h_{ss}) = -\tan(L)\tan(\delta) \tag{2.15}$$

where h_{ss} is taken as positive at sunset.

Since the hour angle at local solar noon is 0°, with each 15° of longitude equivalent to 1 h, the sunrise and sunset time in hours from local solar noon is then:

$$H_{ss} = -H_{sr} = 1/15\ \cos^{-1}\left[-\tan(L)\tan(\delta)\right] \tag{2.16}$$

The sunrise and sunset hour angles for various latitudes are shown in Figure A3.1 in Appendix 3.

The day length is twice the sunset hour, since the solar noon is at the middle of the sunrise and sunset hours. Therefore, the length of the day in hours is:

$$\text{Day length} = 2/15\ \cos^{-1}\left[-\tan(L)\tan(\delta)\right] \tag{2.17}$$

EXAMPLE 2.5

Find the equation for sunset standard time for Nicosia, Cyprus.

Solution

The LST at sunset for the location of Nicosia, Cyprus, from Example 2.1 is:

$$\text{Sunset standard time} = H_{ss} - \text{ET} - 13.32\ (\text{min})$$

EXAMPLE 2.6

Find the solar altitude and azimuth angles at 2 h after local noon on June 16 for a city located at 40°N latitude. Also find the sunrise and sunset hours and the day length.

Solution

From Eq. (2.5), the declination on June 16 ($N = 167$) is:

$$\delta = 23.45 \sin\left[\frac{360}{365}(284 + 167)\right] = 23.35^\circ$$

From Eq. (2.8), the hour angle, 2 h after local solar noon is:

$$h = +0.25(120) = 30^\circ$$

From Eq. (2.12), the solar altitude angle is:

$$\sin(\alpha) = \sin(40)\sin(23.35) + \cos(40)\cos(23.35)\cos(30) = 0.864$$

Therefore,

$$\alpha = 59.75^\circ$$

From Eq. (2.13), the solar azimuth angle is:

$$\sin(z) = \cos(23.35)\frac{\sin(30)}{\cos(59.75)} = 0.911$$

Therefore,

$$z = 65.67^\circ$$

From Eq. (2.17), the day length is:

$$\text{Day length} = 2/15 \cos^{-1}\left[-\tan(40)\tan(23.35)\right] = 14.83 \text{ h}$$

This means that the sun rises at $12 - 7.4 = 4.6 = 4{:}36$ am solar time and sets at $7.4 = 7{:}24$ pm solar time.

Incidence angle, θ

The solar incidence angle, θ, is the angle between the sun's rays and the normal on a surface. For a horizontal plane, the incidence angle, θ, and the zenith angle, Φ, are the same. The angles shown in Figure 2.9 are related to the basic angles, shown in Figure 2.5, with the following general expression for the angle of incidence (Kreith and Kreider, 1978; Duffie and Beckman, 1991):

$$\begin{aligned}\cos(\theta) = {} & \sin(L)\sin(\delta)\cos(\beta) - \cos(L)\sin(\delta)\sin(\beta)\cos(Z_s) \\ & + \cos(L)\cos(\delta)\cos(h)\cos(\beta) \\ & + \sin(L)\cos(\delta)\cos(h)\sin(\beta)\cos(Z_s) \\ & + \cos(\delta)\sin(h)\sin(\beta)\sin(Z_s)\end{aligned} \tag{2.18}$$

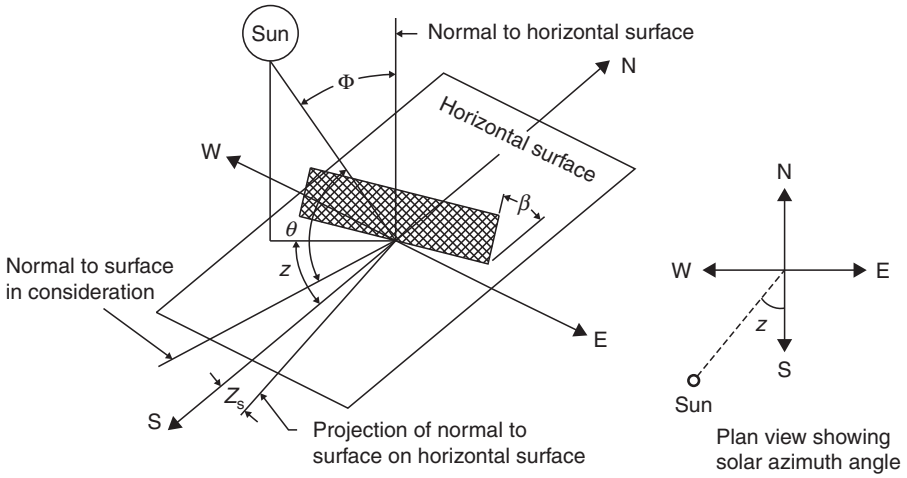

FIGURE 2.9

Solar angles diagram.

where

$\beta =$ surface tilt angle from the horizontal,
$Z_s =$ surface azimuth angle, the angle between the normal to the surface from true south, westward is designated as positive.

For certain cases Eq. (2.18) reduces to much simpler forms:

- *For horizontal surfaces*, $\beta = 0°$ and $\theta = \Phi$, and Eq. (2.18) reduces to Eq. (2.12).
- *For vertical surfaces*, $\beta = 90°$ and Eq. (2.18) becomes:

$$\cos(\theta) = -\cos(L)\sin(\delta)\cos(Z_s) + \sin(L)\cos(\delta)\cos(h)\cos(Z_s) + \cos(\delta)\sin(h)\sin(Z_s) \tag{2.19}$$

- *For a south-facing tilted surface in the Northern Hemisphere*, $Z_s = 0°$ and Eq. (2.18) reduces to:

$$\begin{aligned}\cos(\theta) = {} & \sin(L)\sin(\delta)\cos(\beta) - \cos(L)\sin(\delta)\sin(\beta) \\ & + \cos(L)\cos(\delta)\cos(h)\cos(\beta) + \sin(L)\cos(\delta)\cos(h)\sin(\beta)\end{aligned}$$

  which can be further reduced to:

$$\cos(\theta) = \sin(L-\beta)\sin(\delta) + \cos(L-\beta)\cos(\delta)\cos(h) \tag{2.20}$$

- *For a north-facing tilted surface in the Southern Hemisphere*, $Z_s = 180°$ and Eq. (2.18) reduces to:

$$\cos(\theta) = \sin(L+\beta)\sin(\delta) + \cos(L+\beta)\cos(\delta)\cos(h) \tag{2.21}$$

Equation (2.18) is a general relationship for the angle of incidence on a surface of any orientation. As shown in Eqs (2.19)–(2.21), it can be reduced to much simpler forms for specific cases.

EXAMPLE 2.7

A surface tilted 45° from horizontal and pointed 10° west of due south is located at 35°N latitude. Calculate the incident angle at 2 h after local noon on June 16.

Solution

From Example 2.6 we have $\delta = 23.35°$ and the hour angle $= 30°$. The solar incidence angle θ is calculated from Eq. (2.18):

$$\begin{aligned}\cos(\theta) &= \sin(35)\sin(23.35)\cos(45) - \cos(35)\sin(23.35)\sin(45)\cos(10)\\ &\quad + \cos(35)\cos(23.35)\cos(30)\cos(45) + \sin(35)\cos(23.35)\cos(30)\sin(45)\cos(10)\\ &\quad + \cos(23.35)\sin(30)\sin(45)\sin(10)\\ &= 0.769\end{aligned}$$

Therefore,

$$\theta = 39.72°$$

2.2.1 The incidence angle for moving surfaces

For the case of solar-concentrating collectors, some form of tracking mechanism is usually employed to enable the collector to follow the sun. This is done with varying degrees of accuracy and modes of tracking, as indicated in Figure 2.10.

Tracking systems can be classified by the mode of their motion. This can be about a single axis or about two axes (Figure 2.10(a)). In the case of a single-axis mode, the motion can be in various ways: parallel to the earth's axis (Figure 2.10(b)), north–south (Figure 2.10(c)), or east–west (Figure 2.10(d)). The following equations are derived from the general Eq. (2.18) and apply to planes moved, as indicated in each case. The amount of energy falling on a surface per unit area for the summer and winter solstices and the equinoxes for latitude of 35°N is investigated for each mode. This analysis has been performed with a radiation model. This is affected by the incidence angle, which is different for each mode. The type of model used here is not important, since it is used for comparison purposes only.

Full tracking

For a two-axis tracking mechanism, keeping the surface in question continuously oriented to face the sun (see Figure 2.10(a)) at all times has an angle of incidence, θ, equal to:

$$\cos(\theta) = 1 \tag{2.22}$$

or $\theta = 0°$. This, of course, depends on the accuracy of the mechanism. The full tracking configuration collects the maximum possible sunshine. The performance of this mode of tracking with respect to the amount of radiation collected during one day under standard conditions is shown in Figure 2.11.

The slope of this surface (β) is equal to the solar zenith angle (Φ), and the surface azimuth angle (Z_s) is equal to the solar azimuth angle (z).

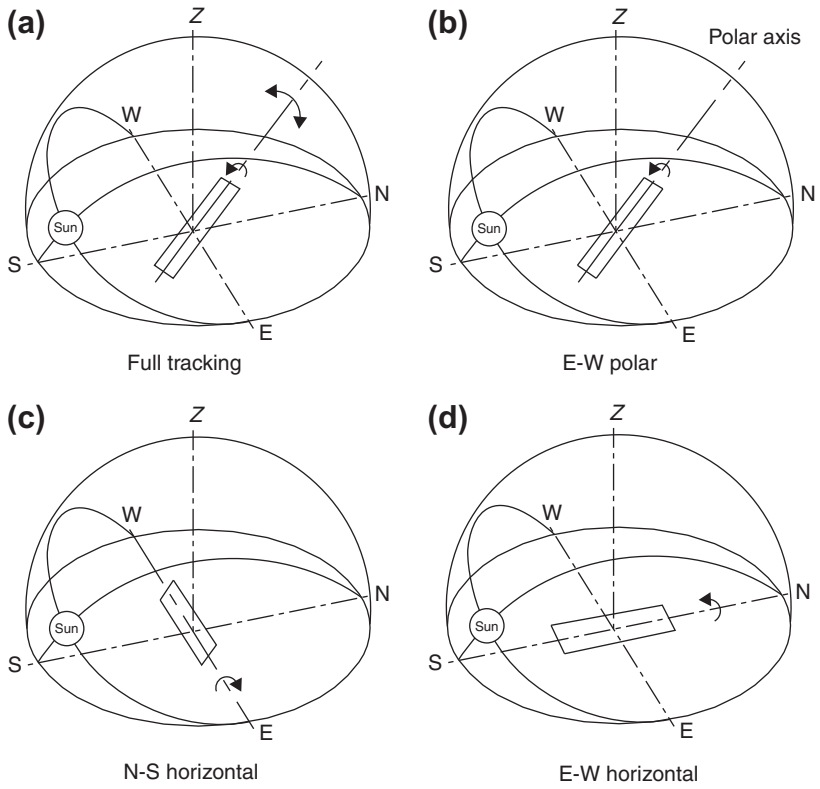

FIGURE 2.10

Collector geometry for various modes of tracking.

Tilted N–S axis with tilt adjusted daily

For a plane moved about a north–south axis with a single daily adjustment so that its surface normal coincides with the solar beam at noon each day, θ is equal to (Meinel and Meinel, 1976; Duffie and Beckman, 1991):

$$\cos(\theta) = \sin^2(\delta) + \cos^2(\delta)\cos(h) \tag{2.23}$$

For this mode of tracking, we can accept that, when the sun is at noon, the angle of the sun's rays and the normal to the collector can be up to a 4° declination, since for small angles $\cos(4°) = 0.998 \sim 1$. Figure 2.12 shows the number of consecutive days that the sun remains within this 4° "declination window" at noon. As can be seen in Figure 2.12, most of the time the sun remains close to either the summer solstice or the winter solstice, moving rapidly between the two extremes. For nearly 70 consecutive days, the sun is within 4° of an extreme position, spending only 9 days in the 4° window, at the equinox. This means that a seasonally tilted collector needs to be adjusted only occasionally.

The problem encountered with this and all tilted collectors, when more than one collector is used, is that the front collectors cast shadows on adjacent ones. Therefore, in terms of land utilization, these

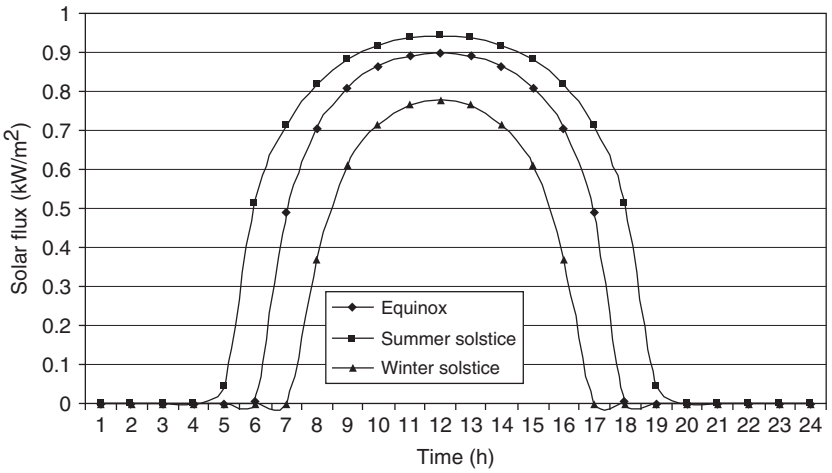

FIGURE 2.11

Daily variation of solar flux, full tracking.

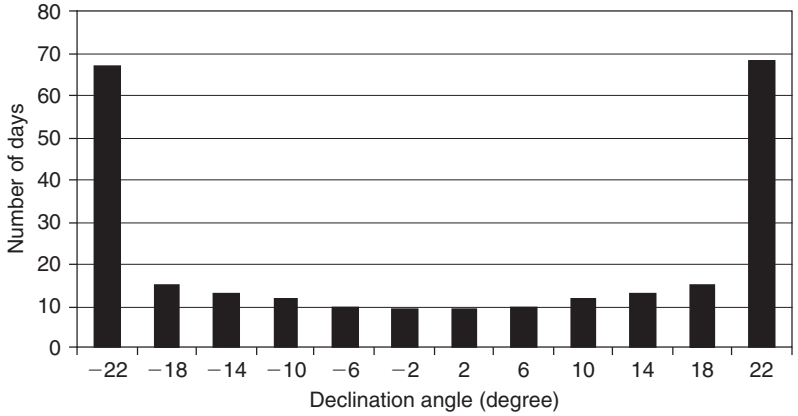

FIGURE 2.12

Number of consecutive days the sun remains within 4° declination.

collectors lose some of their benefits when the cost of land is taken into account. The performance of this mode of tracking (see Figure 2.13) shows the peaked curves typical for this assembly.

Polar N–S axis with E–W tracking

For a plane rotated about a north–south axis parallel to the earth's axis, with continuous adjustment, θ is equal to:

$$\cos(\theta) = \cos(\delta) \tag{2.24}$$

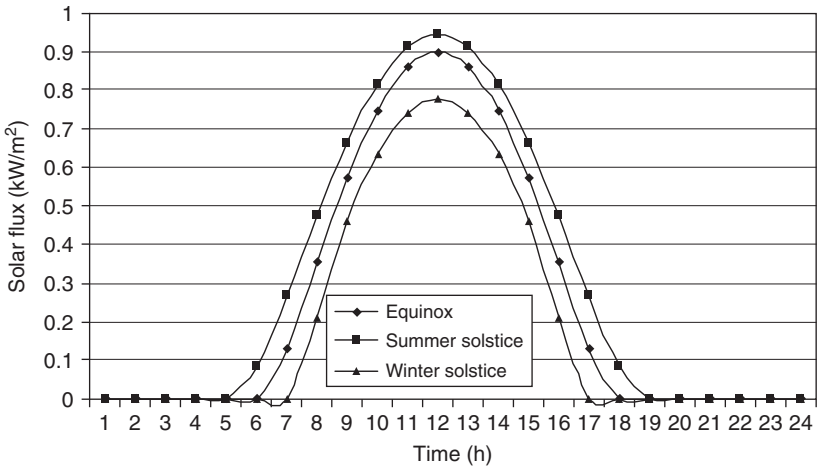

FIGURE 2.13

Daily variation of solar flux: tilted N–S axis with tilt adjusted daily.

This configuration is shown in Figure 2.10(b). As can be seen, the collector axis is tilted at the polar axis, which is equal to the local latitude. For this arrangement, the sun is normal to the collector at equinoxes ($\delta = 0°$) and the cosine effect is maximum at the solstices. The same comments about the tilting of the collector and shadowing effects apply here as in the previous configuration. The performance of this mount is shown in Figure 2.14.

The equinox and summer solstice performance, in terms of solar radiation collected, are essentially equal; that is, the smaller air mass for summer solstice offsets the small cosine projection effect. The winter noon value, however, is reduced because these two effects combine. If it is desired to increase

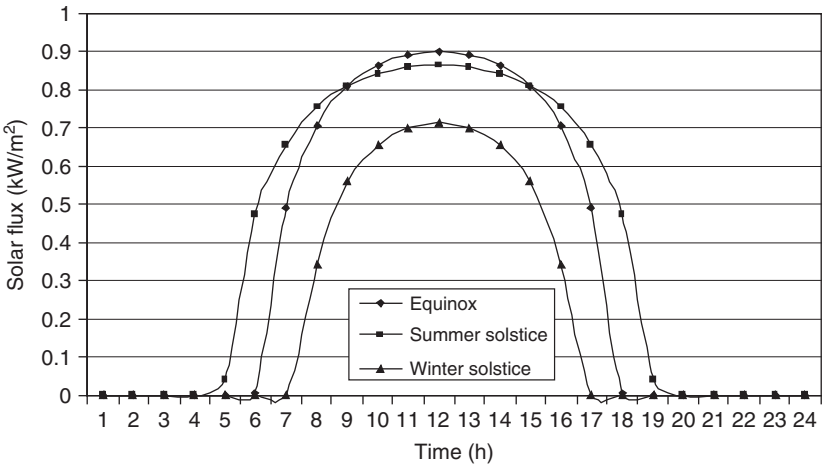

FIGURE 2.14

Daily variation of solar flux: polar N–S axis with E–W tracking.

the winter performance, an inclination higher than the local latitude would be required; but the physical height of such configuration would be a potential penalty to be traded off in cost-effectiveness with the structure of the polar mount. Another side effect of increased inclination is shadowing by the adjacent collectors, for multi-row installations.

The slope of the surface varies continuously and is given by:

$$\tan(\beta) = \frac{\tan(L)}{\cos(Z_s)} \tag{2.25a}$$

The surface azimuth angle is given by:

$$Z_s = \tan^{-1}\frac{\sin(\Phi)\sin(z)}{\cos(\theta')\sin(L)} + 180C_1C_2 \tag{2.25b}$$

where

$$\cos(\theta') = \cos(\Phi)\cos(L) + \sin(\Phi)\sin(L)\cos(z) \tag{2.25c}$$

$$C_1 = \begin{cases} 0 & \text{if} \quad \left(\tan^{-1}\dfrac{\sin(\Phi)\sin(z)}{\cos(\theta')\sin(L)}\right) z \geq 0 \\ 1 & \text{otherwise} \end{cases} \tag{2.25d}$$

$$C_2 = \begin{cases} 1 & \text{if} \quad z \geq 0^\circ \\ -1 & \text{if} \quad z < 0^\circ \end{cases} \tag{2.25e}$$

Horizontal E–W axis with N–S tracking

For a plane rotated about a horizontal east–west axis with continuous adjustment to minimize the-angle of incidence, θ can be obtained from (Kreith and Kreider, 1978; Duffie and Beckman, 1991):

$$\cos(\theta) = \sqrt{1 - \cos^2(\delta)\sin^2(h)} \tag{2.26a}$$

or from this equation (Meinel and Meinel, 1976):

$$\cos(\theta) = \sqrt{\sin^2(\delta) + \cos^2(\delta)\cos^2(h)} \tag{2.26b}$$

The basic geometry of this configuration is shown in Figure 2.10(c). The shadowing effects of this arrangement are minimal. The principal shadowing is caused when the collector is tipped to a maximum degree south ($\delta = -23.5^\circ$) at winter solstice. In this case, the sun casts a shadow toward the collector at the north. This assembly has an advantage in that it approximates the full tracking collector in summer (see Figure 2.15), but the cosine effect in winter greatly reduces its effectiveness. This mount yields a rather "square" profile of solar radiation, ideal for leveling the variation during the day. The winter performance, however, is seriously depressed relative to the summer one.

The slope of this surface is given by:

$$\tan(\beta) = \tan(\Phi)|\cos(z)| \tag{2.27a}$$

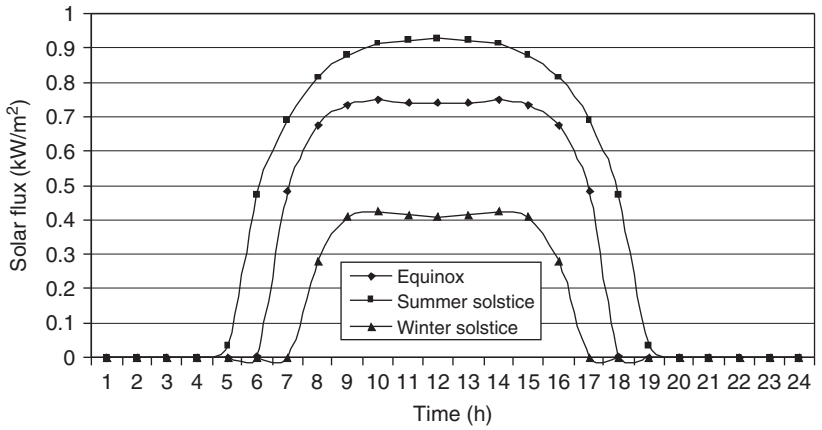

FIGURE 2.15

Daily variation of solar flux: horizontal E–W axis with N–S tracking.

The surface orientation for this mode of tracking changes between 0° and 180°, if the solar azimuth angle passes through ±90°. For either hemisphere,

$$\begin{aligned} &\text{If } |z| < 90^\circ, \ Z_s = 0^\circ \\ &\text{If } |z| > 90^\circ, \ Z_s = 180^\circ \end{aligned} \tag{2.27b}$$

Horizontal N–S axis with E–W tracking

For a plane rotated about a horizontal north–south axis with continuous adjustment to minimize the angle of incidence, θ can be obtained from (Kreith and Kreider, 1978; Duffie and Beckman, 1991),

$$\cos(\theta) = \sqrt{\sin^2(\alpha) + \cos^2(\delta)\sin^2(h)} \tag{2.28a}$$

or from this equation (Meinel and Meinel, 1976):

$$\cos(\theta) = \cos(\Phi)\cos(h) + \cos(\delta)\sin^2(h) \tag{2.28b}$$

The basic geometry of this configuration is shown in Figure 2.10(d). The greatest advantage of this arrangement is that very small shadowing effects are encountered when more than one collector is used. These are present only at the first and last hours of the day. In this case the curve of the solar energy collected during the day is closer to a cosine curve function (see Figure 2.16).

The slope of this surface is given by:

$$\tan(\beta) = \tan(\Phi)|\cos(Z_s - z)| \tag{2.29a}$$

The surface azimuth angle (Z_s) is 90° or −90°, depending on the solar azimuth angle:

$$\begin{aligned} &\text{If } z > 0^\circ, \ Z_s = 90^\circ \\ &\text{If } z < 0^\circ, \ Z_s = -90^\circ \end{aligned} \tag{2.29b}$$

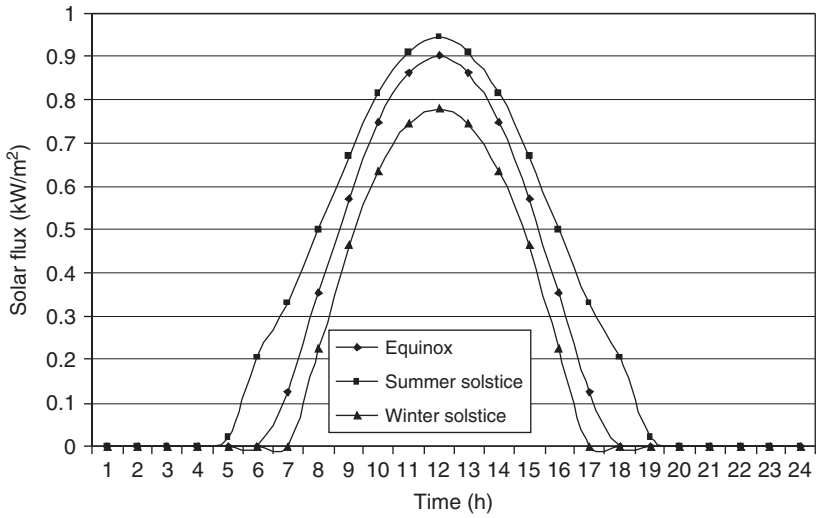

FIGURE 2.16

Daily variation of solar flux: horizontal N–S axis and E–W tracking.

Comparison

The mode of tracking affects the amount of incident radiation falling on the collector surface in proportion to the cosine of the incidence angle. The amount of energy falling on a surface per unit area for the four modes of tracking for the summer and winter solstices and the equinoxes are shown in Table 2.2. This analysis has been performed with the same radiation model used to plot the solar flux figures in this section. Again, the type of the model used here is not important, because it is used for comparison purposes only. The performance of the various modes of tracking is compared with the full tracking, which collects the maximum amount of solar energy, shown as 100% in Table 2.2. From this table it is obvious that the polar and the N–S horizontal modes are the most suitable for one-axis

Table 2.2 Comparison of Energy Received for Various Modes of Tracking

	Solar Energy Received (kWh/m^2)			Percentage to Full Tracking		
Tracking Mode	**E**	**SS**	**WS**	**E**	**SS**	**WS**
Full tracking	8.43	10.60	5.70	100	100	100
E–W polar	8.43	9.73	5.23	100	91.7	91.7
N–S horizontal	7.51	10.36	4.47	89.1	97.7	60.9
E–W horizontal	6.22	7.85	4.91	73.8	74.0	86.2

E = equinoxes, SS = summer solstice, WS = winter solstice.

tracking, since their performance is very close to the full tracking, provided that the low winter performance of the latter is not a problem.

2.2.2 Sun path diagrams

For practical purposes, instead of using the preceding equations, it is convenient to have the sun's path plotted on a horizontal plane, called a *sun path diagram*, and to use the diagram to find the position of the sun in the sky at any time of the year. As can be seen from Eqs (2.12) and (2.13), the solar altitude angle, α, and the solar azimuth angle, z, are functions of latitude, L, hour angle, h, and declination, δ. In a two-dimensional plot, only two independent parameters can be used to correlate the other parameters; therefore, it is usual to plot different sun path diagrams for different latitudes. Such diagrams show the complete variations of hour angle and declination for a full year. Figure 2.17 shows the sun path diagram for 35°N latitude. Lines of constant declination are labeled by the value of the angles. Points of constant hour angles are clearly indicated. This figure is used in combination with Figure 2.7 or Eqs (2.5)–(2.7); that is, for a day in a year, Figure 2.7 or the equations can be used to estimate declination, which is then entered together with the time of day and converted to solar time using Eq. (2.3) in Figure 2.17 to estimate solar altitude and azimuth angles. It should be noted that Figure 2.17 applies for the Northern Hemisphere. For the Southern Hemisphere, the sign of the declination should be reversed. Figures A3.2 through A3.4 in Appendix 3 show the sun path diagrams for 30°, 40°, and 50°N latitudes.

2.2.3 Shadow determination

In the design of many solar energy systems, it is often required to estimate the possibility of the shading of solar collectors or the windows of a building by surrounding structures. To determine the shading, it is necessary to know the shadow cast as a function of time during every day of the year. Although mathematical models can be used for this purpose, a simpler graphical method is presented here, which is suitable for quick practical applications. This method is usually sufficient, since the objective is usually not to estimate exactly the amount of shading but to determine whether a position suggested for the placement of collectors is suitable or not.

Shadow determination is facilitated by the determination of a surface-oriented solar angle, called the *solar profile angle*. As shown in Figure 2.18, the solar profile angle, p, is the angle between the normal to a surface and the projection of the sun's rays on a plane normal to the surface. In terms of the solar altitude angle, α, solar azimuth angle, z, and the surface azimuth angle, Z_s, the solar profile angle p is given by the equation:

$$\tan(p) = \frac{\tan(\alpha)}{\cos(z - Z_s)} \tag{2.30a}$$

A simplified equation is obtained when the surface faces due south, that is, $Z_s = 0°$, given by:

$$\tan(p) = \frac{\tan(\alpha)}{\cos(z)} \tag{2.30b}$$

The sun path diagram is often very useful in determining the period of the year and hours of day when shading will take place at a particular location. This is illustrated in the following example.

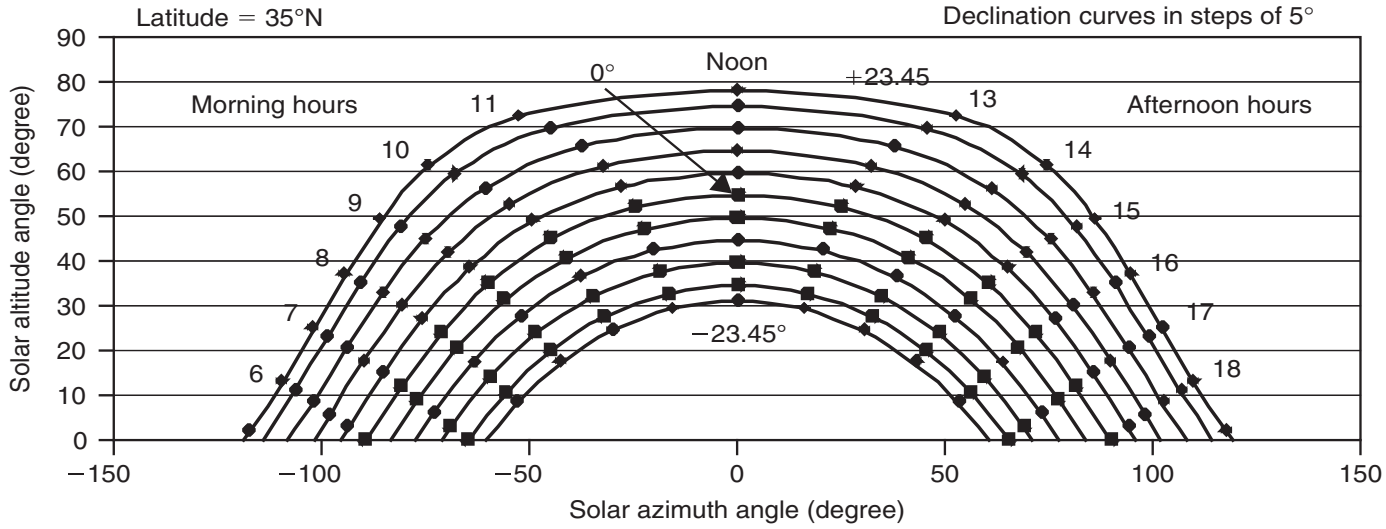

FIGURE 2.17

Sun path diagram for 35°N latitude.

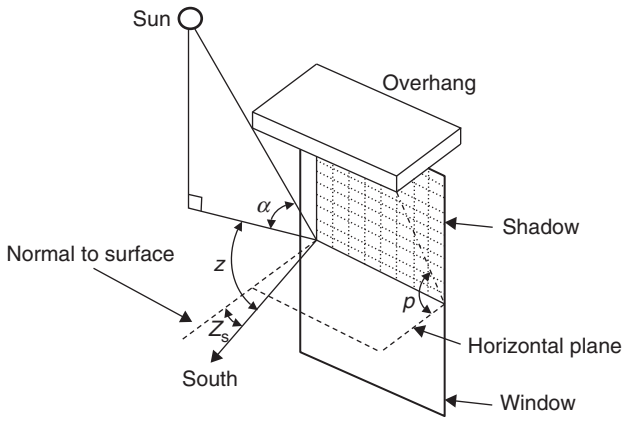

FIGURE 2.18

Geometry of solar profile angle, *p*, in a window overhang arrangement.

EXAMPLE 2.8

A building is located at 35°N latitude and its side of interest is located 15° east of south. We want to investigate the time of the year that point *x* on the building will be shaded, as shown in Figure 2.19.

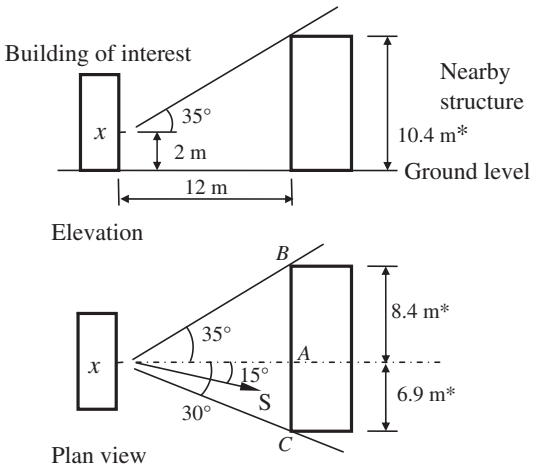

Note: Distances marked with * can also be obtained from simple trigonometry

FIGURE 2.19

Shading of building in Example 2.8.

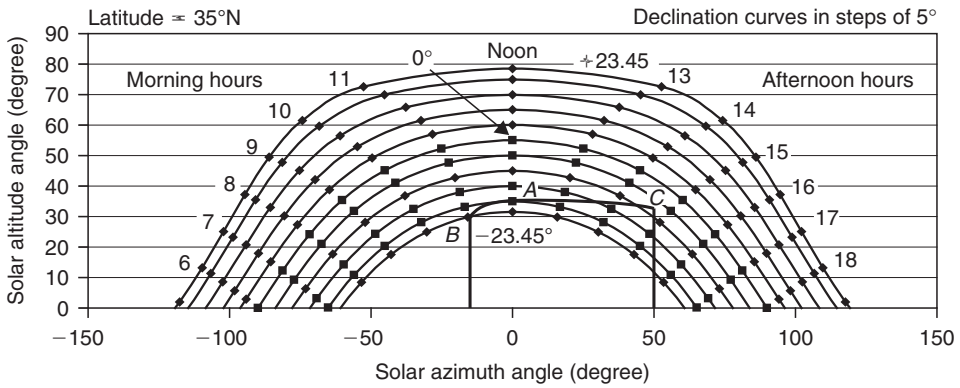

FIGURE 2.20

Sun path diagram for Example 2.8.

Solution

The upper limit of profile angle for shading point x is 35° and 15° west of true south. This is point A drawn on the sun path diagram, as shown in Figure 2.20. In this case, the solar profile angle is the solar altitude angle. Distance x–B is $(8.4^2 + 12^2)^{1/2} = 14.6$ m. For the point B, the altitude angle is $\tan(\alpha) = 8.4/14.6 \rightarrow \alpha = 29.9°$. Similarly, distance x–C is $(6.9^2 + 12^2)^{1/2} = 13.8$ m, and for point C, the altitude angle is $\tan(\alpha) = 8.4/13.8 \rightarrow \alpha = 31.3°$. Both points are as indicated on the sun path diagram in Figure 2.20.

Therefore, point x on the wall of interest is shaded during the period indicated by the curve BAC in Figure 2.20. It is straightforward to determine the hours that shading occurs, whereas the time of year is determined by the declination.

Solar collectors are usually installed in multi-rows facing the true south. There is, hence, a need to estimate the possibility of shading by the front rows of the second and subsequent rows. The maximum shading, in this case, occurs at local solar noon, and this can easily be estimated by finding the noon altitude, α_n, as given by Eq. (2.14) and checking whether the shadow formed shades on the second or subsequent collector rows. Generally, shading will not occur as long as the profile angle is greater than the angle θ_s, formed by the top corner of the front collector to the bottom end of the second row and the horizontal (see Figure 5.25). If the profile angle at any time is less than θ_s, then a portion of the collectors in the second and subsequent rows will be shaded from beam radiation.

EXAMPLE 2.9

Find the equation to estimate the shading caused by a fin on a window.

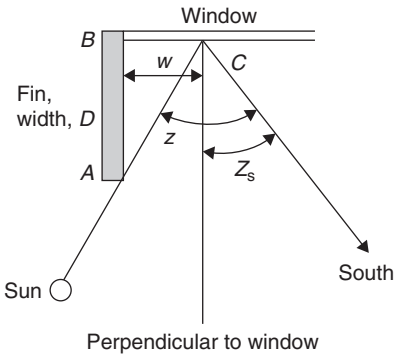

FIGURE 2.21

Fin and window assembly for Example 2.9.

Solution

The fin and window assembly are shown in Figure 2.21.

From triangle ABC, the sides $AB = D$, $BC = w$, and angle A is $z - Z_s$.

Therefore, distance w is estimated by $w = D \tan(z - Z_s)$.

Shadow calculations for overhangs are examined in more detail in Chapter 6, Section 6.2.5.

2.3 Solar radiation

2.3.1 General

All substances, solid bodies as well as liquids and gases above the absolute zero temperature, emit energy in the form of electromagnetic waves.

The radiation that is important to solar energy applications is that emitted by the sun within the ultraviolet, visible, and infrared regions. Therefore, the radiation wavelength that is important to solar energy applications is between 0.15 and 3.0 μm. The wavelengths in the visible region lie between 0.38 and 0.72 μm.

This section initially examines issues related to thermal radiation, which includes basic concepts, radiation from real surfaces, and radiation exchanges between two surfaces. This is followed by the variation of extraterrestrial radiation, atmospheric attenuation, terrestrial irradiation, and total radiation received on sloped surfaces. Finally, it briefly describes radiation measuring equipment.

2.3.2 Thermal radiation

Thermal radiation is a form of energy emission and transmission that depends entirely on the temperature characteristics of the emissive surface. There is no intervening carrier, as in the other modes of

heat transmission, that is, conduction and convection. Thermal radiation is in fact an electromagnetic wave that travels at the speed of light ($C \approx 300{,}000$ km/s in a vacuum). This speed is related to the wavelength (λ) and frequency (ν) of the radiation as given by the equation:

$$C = \lambda \nu \tag{2.31}$$

When a beam of thermal radiation is incident on the surface of a body, part of it is reflected away from the surface, part is absorbed by the body, and part is transmitted through the body. The various properties associated with this phenomenon are the fraction of radiation reflected, called *reflectivity* (ρ); the fraction of radiation absorbed, called *absorptivity* (α); and the fraction of radiation transmitted, called *transmissivity* (τ). The three quantities are related by the following equation:

$$\rho + \alpha + \tau = 1 \tag{2.32}$$

It should be noted that the radiation properties just defined are not only functions of the surface itself but also functions of the direction and wavelength of the incident radiation. Therefore, Eq. (2.32) is valid for the average properties over the entire wavelength spectrum. The following equation is used to express the dependence of these properties on the wavelength:

$$\rho_\lambda + \alpha_\lambda + \tau_\lambda = 1 \tag{2.33}$$

where

ρ_λ = spectral reflectivity.
α_λ = spectral absorptivity.
τ_λ = spectral transmissivity.

The angular variation of absorptance for black paint is illustrated in Table 2.3 for incidence angles of 0–90°. The absorptance for diffuse radiation is approximately 0.90 (Löf and Tybout, 1972).

Most solid bodies are opaque, so that $\tau = 0$ and $\rho + \alpha = 1$. If a body absorbs all the impinging thermal radiation such that $\tau = 0$, $\rho = 0$, and $\alpha = 1$, regardless of the spectral character or directional preference of the incident radiation, it is called a *blackbody*. This is a hypothetical idealization that does not exist in reality.

Table 2.3 Angular Variation of Absorptance for Black Paint

Angle of Incidence (°)	Absorptance
0–30	0.96
30–40	0.95
40–50	0.93
50–60	0.91
60–70	0.88
70–80	0.81
80–90	0.66

Reprinted from Löf and Tybout (1972) with permission from ASME.

A blackbody is not only a perfect absorber but also characterized by an upper limit to the emission of thermal radiation. The energy emitted by a blackbody is a function of its temperature and is not evenly distributed over all wavelengths. The rate of energy emission per unit area at a particular wavelength is termed as the *monochromatic emissive power*. Max Planck was the first to derive a functional relation for the monochromatic emissive power of a blackbody in terms of temperature and wavelength. This was done by using the quantum theory, and the resulting equation, called *Planck's equation for blackbody radiation*, is given by:

$$E_{b\lambda} = \frac{C_1}{\lambda^5\left(e^{C_2/\lambda T} - 1\right)} \tag{2.34}$$

where

$E_{b\lambda}$ = monochromatic emissive power of a blackbody (W/m^2 μm).
T = absolute temperature of the surface (K).
λ = wavelength (μm).
C_1 = constant = $2\pi hc_o^2 = 3.74177 \times 10^8$ W μm^4/m^2.
C_2 = constant = $hc_o/k = 1.43878 \times 10^4$ μm K.
h = Planck's constant = 6.626069×10^{-34} Js.
c_o = speed of light in vacuum = 2.9979×10^8 m/s.
k = Boltzmann's constant = 1.38065×10^{-23} J/K.

Equation (2.34) is valid for a surface in a vacuum or a gas. For other mediums it needs to be modified by replacing C_1 by C_1/n^2, where n is the index of refraction of the medium. By differentiating Eq. (2.34) and equating to 0, the wavelength corresponding to the maximum of the distribution can be obtained and is equal to $\lambda_{max}T = 2897.8$ μm K. This is known as *Wien's displacement law*. Figure 2.22 shows the spectral radiation distribution for blackbody radiation at three temperature sources. The curves have been obtained by using the Planck's equation.

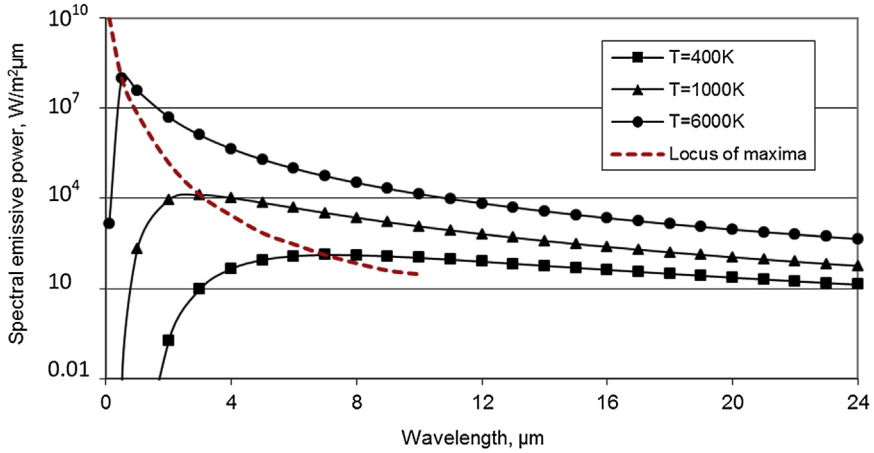

FIGURE 2.22

Spectral distribution of blackbody radiation.

The total emissive power, E_b, and the monochromatic emissive power, $E_{b\lambda}$, of a blackbody are related by:

$$E_b = \int_0^\infty E_{b\lambda}\, d\lambda \tag{2.35}$$

Substituting Eq. (2.34) into Eq. (2.35) and performing the integration results in the Stefan–Boltzmann law:

$$E_b = \sigma T^4 \tag{2.36a}$$

where σ = the Stefan–Boltzmann constant = 5.6697×10^{-8} W/m^{2}K^4.

In many cases, it is necessary to know the amount of radiation emitted by a blackbody in a specific wavelength band $\lambda_1 \rightarrow \lambda_2$. This is done by modifying Eq. (2.35) as:

$$E_b(0 \rightarrow \lambda) = \int_0^\lambda E_{b\lambda}\, d\lambda \tag{2.36b}$$

Since the value of $E_{b\lambda}$ depends on both λ and T, it is better to use both variables as:

$$E_b(0 \rightarrow \lambda T) = \int_0^{\lambda T} \frac{E_{b\lambda}}{T}\, d\lambda T \tag{2.36c}$$

Therefore, for the wavelength band of $\lambda_1 \rightarrow \lambda_2$, we get:

$$E_b(\lambda_1 T \rightarrow \lambda_2 T) = \int_{\lambda_1 T}^{\lambda_2 T} \frac{E_{b\lambda}}{T}\, d\lambda T \tag{2.36d}$$

which results in $E_b(0 \rightarrow \lambda_1 T) - E_b(0 \rightarrow \lambda_2 T)$. Table 2.4 presents a tabulation of $E_b(0 \rightarrow \lambda T)$ as a fraction of the total emissive power, $E_b = \sigma T^4$, for various values of λT, also called *fraction of radiation emitted* from a blackbody at temperature T in the wavelength band from $\lambda = 0$ to λ, $f_{0\text{-}\lambda T}$ or for a particular temperature, f_λ. The values are not rounded, because the original table, suggested by Dunkle (1954), recorded λT in micrometer-degrees Rankine (μm °R), which were converted to micrometer-Kelvins (μm K) in Table 2.4.

The fraction of radiation emitted from a blackbody at temperature T in the wavelength band from $\lambda = 0$ to λ can be solved easily on a computer using the polynomial form, with about 10 summation terms for good accuracy, suggested by Siegel and Howell (2002):

$$f_{0\text{-}\lambda T} = \frac{15}{\pi^4} \sum_{n=1}^{\infty} \left[\frac{e^{-n\omega}}{n} \left(\omega^3 + \frac{3\omega^2}{n} + \frac{6\omega}{n^2} + \frac{6}{n^3} \right) \right] \tag{2.36e}$$

where $\omega = C_2/\lambda T$

Table 2.4 Fraction of Blackbody Radiation as a Function of λT

λT (μm K)	$E_b(0 \rightarrow \lambda T)/\sigma T^4$	λT (μm K)	$E_b(0 \rightarrow \lambda T)/\sigma T^4$	λT (μm K)	$E_b(0 \rightarrow \lambda T)/\sigma T^4$
555.6	1.70E−08	4000.0	0.48085	7444.4	0.83166
666.7	7.56E−07	4111.1	0.50066	7555.6	0.83698
777.8	1.06E−05	4222.2	0.51974	7666.7	0.84209
888.9	7.38E−05	4333.3	0.53809	7777.8	0.84699
1000.0	3.21E−04	4444.4	0.55573	7888.9	0.85171
1111.1	0.00101	4555.6	0.57267	8000.0	0.85624
1222.2	0.00252	4666.7	0.58891	8111.1	0.86059
1333.3	0.00531	4777.8	0.60449	8222.2	0.86477
1444.4	0.00983	4888.9	0.61941	8333.3	0.86880
1555.6	0.01643	5000.0	0.63371	8888.9	0.88677
1666.7	0.02537	5111.1	0.64740	9444.4	0.90168
1777.8	0.03677	5222.2	0.66051	10,000.0	0.91414
1888.9	0.05059	5333.3	0.67305	10,555.6	0.92462
2000.0	0.06672	5444.4	0.68506	11,111.1	0.93349
2111.1	0.08496	5555.6	0.69655	11,666.7	0.94104
2222.2	0.10503	5666.7	0.70754	12,222.2	0.94751
2333.3	0.12665	5777.8	0.71806	12,777.8	0.95307
2444.4	0.14953	5888.9	0.72813	13,333.3	0.95788
2555.5	0.17337	6000.0	0.73777	13,888.9	0.96207
2666.7	0.19789	6111.1	0.74700	14,444.4	0.96572
2777.8	0.22285	6222.1	0.75583	15,000.0	0.96892
2888.9	0.24803	6333.3	0.76429	15,555.6	0.97174
3000.0	0.27322	6444.4	0.77238	16,111.1	0.97423
3111.1	0.29825	6555.6	0.78014	16,666.7	0.97644
3222.2	0.32300	6666.7	0.78757	22,222.2	0.98915
3333.3	0.34734	6777.8	0.79469	22,777.8	0.99414
3444.4	0.37118	6888.9	0.80152	33,333.3	0.99649
3555.6	0.39445	7000.0	0.80806	33,888.9	0.99773
3666.7	0.41708	7111.1	0.81433	44,444.4	0.99845
3777.8	0.43905	7222.2	0.82035	50,000.0	0.99889
3888.9	0.46031	7333.3	0.82612	55,555.6	0.99918

A blackbody is also a perfect diffuse emitter, so its intensity of radiation, I_b, is a constant in all directions, given by:

$$E_b = \pi I_b \tag{2.37}$$

Of course, real surfaces emit less energy than corresponding blackbodies. The ratio of the total emissive power, E, of a real surface to the total emissive power, E_b, of a blackbody, both at the same temperature, is called the *emissivity* (ε) of a real surface; that is,

$$\varepsilon = \frac{E}{E_b} \tag{2.38}$$

The emissivity of a surface not only is a function of surface temperature but also depends on wavelength and direction. In fact, the emissivity given by Eq. (2.38) is the average value over the entire wavelength range in all directions, and it is often referred to as the *total* or *hemispherical emissivity*. Similar to Eq. (2.38), to express the dependence on wavelength, the monochromatic or spectral emissivity, ε_λ, is defined as the ratio of the monochromatic emissive power, E_λ, of a real surface to the monochromatic emissive power, $E_{b\lambda}$, of a blackbody, both at the same wavelength and temperature:

$$\varepsilon_\lambda = \frac{E_\lambda}{E_{b\lambda}} \tag{2.39}$$

Kirchoff's law of radiation states that, for any surface in thermal equilibrium, monochromatic emissivity is equal to monochromatic absorptivity:

$$\varepsilon_\lambda(T) = \alpha_\lambda(T) \tag{2.40}$$

The temperature (T) is used in Eq. (2.40) to emphasize that this equation applies only when the temperatures of the source of the incident radiation and the body itself are the same. It should be noted, therefore, that the emissivity of a body on earth (at normal temperature) cannot be equal to solar radiation (emitted from the sun at $T = 5760$ K). Equation (2.40) can be generalized as:

$$\varepsilon(T) = \alpha(T) \tag{2.41}$$

Equation (2.41) relates the total emissivity and absorptivity over the entire wavelength. This generalization, however, is strictly valid only if the incident and emitted radiation have, in addition to the temperature equilibrium at the surfaces, the same spectral distribution. Such conditions are rarely met in real life; to simplify the analysis of radiation problems, however, the assumption that monochromatic properties are constant over all wavelengths is often made. Such a body with these characteristics is called a *gray body*.

Similar to Eq. (2.37) for a real surface, the radiant energy leaving the surface includes its original emission and any reflected rays. The rate of total radiant energy leaving a surface per unit surface area is called the *radiosity* (J), given by:

$$J = \varepsilon E_b + \rho H \tag{2.42}$$

where

E_b = blackbody emissive power per unit surface area (W/m^2).
H = irradiation incident on the surface per unit surface area (W/m^2).
ε = emissivity of the surface.
ρ = reflectivity of the surface.

There are two idealized limiting cases of radiation reflection: the reflection is called *specular* if the reflected ray leaves at an angle with the normal to the surface equal to the angle made by the incident ray, and it is called *diffuse* if the incident ray is reflected uniformly in all directions. Real surfaces are neither perfectly specular nor perfectly diffuse. Rough industrial surfaces, however, are often considered as diffuse reflectors in engineering calculations.

A real surface is both a diffuse emitter and a diffuse reflector and hence, it has diffuse radiosity; that is, the intensity of radiation from this surface (I) is constant in all directions. Therefore, the following equation is used for a real surface:

$$J = \pi \times I \tag{2.43}$$

EXAMPLE 2.10

A glass with transmissivity of 0.92 is used in a certain application for wavelengths 0.3 and 3.0 μm. The glass is opaque to all other wavelengths. Assuming that the sun is a blackbody at 5760 K and neglecting atmospheric attenuation, determine the percent of incident solar energy transmitted through the glass. If the interior of the application is assumed to be a blackbody at 373 K, determine the percent of radiation emitted from the interior and transmitted out through the glass.

Solution

For the incoming solar radiation at 5760 K, we have:

$$\lambda_1 T = 0.3 \times 5760 = 1728 \ \mu\text{m K}$$

$$\lambda_2 T = 3 \times 5760 = 17280 \ \mu\text{m K}$$

From Table 2.4 by interpolation, we get:

$$\frac{E_b(0 \rightarrow \lambda_1 T)}{\sigma T^4} = 0.0317 = 3.17\%$$

$$\frac{E_b(0 \rightarrow \lambda_2 T)}{\sigma T^4} = 0.9778 = 97.78\%$$

Therefore, the percent of solar radiation incident on the glass in the wavelength range 0.3−3 μm is:

$$\frac{E_b(\lambda_1 T \rightarrow \lambda_2 T)}{\sigma T^4} = 97.78 - 3.17 = 94.61\%$$

In addition, the percentage of radiation transmitted through the glass is $0.92 \times 94.61 = 87.04\%$.

For the outgoing infrared radiation at 373 K, we have:

$$\lambda_1 T = 0.3 \times 373 = 111.9 \ \mu\text{m K}$$

$$\lambda_2 T = 3 \times 373 = 1119.0 \ \mu\text{m K}$$

From Table 2.4, we get:

$$\frac{E_b(0 \rightarrow \lambda_1 T)}{\sigma T^4} = 0.0 = 0\%$$

$$\frac{E_b(0 \rightarrow \lambda_2 T)}{\sigma T^4} = 0.00101 = 0.1\%$$

The percent of outgoing infrared radiation incident on the glass in the wavelength 0.3−3 μm is 0.1%, and the percent of this radiation transmitted out through the glass is only $0.92 \times 0.1 = 0.092\%$. This example, in fact, demonstrates the principle of the greenhouse effect; that is, once the solar energy is absorbed by the interior objects, it is effectively trapped.

EXAMPLE 2.11

A surface has a spectral emissivity of 0.87 at wavelengths less than 1.5 μm, 0.65 at wavelengths between 1.5 and 2.5 μm, and 0.4 at wavelengths longer than 2.5 μm. If the surface is at 1000 K, determine the average emissivity over the entire wavelength and the total emissive power of the surface.

Solution

From the data given, we have:

$$\lambda_1 T = 1.5 \times 1000 = 1500 \ \mu\text{m K}$$

$$\lambda_2 T = 2.5 \times 1000 = 2500 \ \mu\text{m K}$$

From Table 2.4 by interpolation, we get:

$$\frac{E_b(0 \rightarrow \lambda_1 T)}{\sigma T^4} = 0.01313$$

and

$$\frac{E_b(0 \rightarrow \lambda_2 T)}{\sigma T^4} = 0.16144$$

Therefore,

$$\frac{E_b(\lambda_1 T \rightarrow \lambda_2 T)}{\sigma T^4} = 0.16144 - 0.01313 = 0.14831$$

and

$$\frac{E_b(\lambda_2 T \rightarrow \infty)}{\sigma T^4} = 1 - 0.16144 = 0.83856$$

The average emissive power over the entire wavelength is given by:

$$\varepsilon = 0.87 \times 0.01313 + 0.65 \times 0.14831 + 0.4 \times 0.83856 = 0.4432$$

and the total emissive power of the surface is:

$$E = \varepsilon \sigma T^4 = 0.4432 \times 5.67 \times 10^{-8} \times 1000^4 = 25129.4 \ \text{W/m}^2$$

The other properties of the materials can be obtained using the Kirchhoff's law given by Eq. (2.40) or Eq. (2.41) as demonstrated by the following example.

EXAMPLE 2.12

The variation of the spectral absorptivity of an opaque surface is 0.2 up to the wavelength of 2 μm and 0.7 for bigger wavelengths. Estimate the average absorptivity and reflectivity of the surface from radiation emitted from a source at 2500 K. Determine also the average emissivity of the surface at 3000 K.

Solution

At a temperature of 2500 K:

$$\lambda_1 T = (2\ \mu\text{m})(2500\ \text{K}) = 5000\ \mu\text{m K}.$$

Therefore, from Table 2.4: $\dfrac{E_b(0\rightarrow\lambda_1 T)}{\sigma T^4} = f_{\lambda 1} = 0.63371$

The average absorptivity of the surface is:

$$\alpha(T) = \alpha_1 f_{\lambda 1} + \alpha_2(1 - f_{\lambda 1}) = (0.2)(0.63371) + (0.7)(1 - 0.63371) = 0.383$$

As the surface is opaque from Eq. (2.32): $\alpha + \rho = 1$. So, $\rho = 1 - \alpha = 1 - 0.383 = 0.617$.
Using Kirchhoff's law, from Eq. (2.41) $\varepsilon(T) = \alpha(T)$. So the average emissivity of this surface at $T = 3000$ K is:

$$\lambda_1 T = (2\ \mu\text{m})(3000\ \text{K}) = 6000\ \mu\text{m K}.$$

Therefore, from Table 2.4: $\dfrac{E_b(0\rightarrow\lambda_1 T)}{\sigma T^4} = f_{\lambda 1} = 0.73777$

And $\varepsilon(T) = \varepsilon_1 f_{\lambda 1} + \varepsilon_2(1 - f_{\lambda 1}) = (0.2)(0.73777) + (0.7)(1 - 0.73777) = 0.331$.

2.3.3 Transparent plates

When a beam of radiation strikes the surface of a transparent plate at angle θ_1, called the *incidence angle*, as shown in Figure 2.23, part of the incident radiation is reflected and the remainder is refracted, or bent, to angle θ_2, called the *refraction angle*, as it passes through the interface. Angle θ_1 is also equal to the angle at which the beam is specularly reflected from the surface. Angles θ_1 and θ_2 are not equal when the density of the plane is different from that of the medium through which the radiation travels. Additionally, refraction causes the transmitted beam to be bent toward the perpendicular to the surface of higher density. The two angles are related by the Snell's law:

$$n = \frac{n_2}{n_1} = \frac{\sin\theta_1}{\sin\theta_2} \tag{2.44}$$

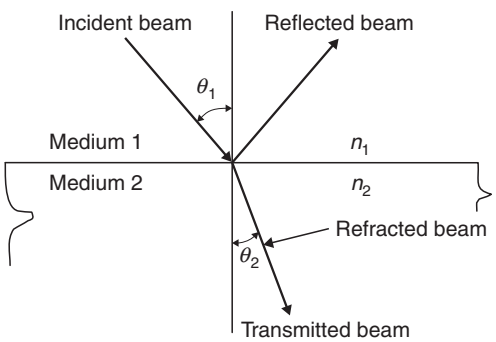

FIGURE 2.23

Incident and refraction angles for a beam passing from a medium with refraction index n_1 to a medium with refraction index n_2.

where n_1 and n_2 are the refraction indices and n is the ratio of refraction index for the two media forming the interface. The refraction index is the determining factor for the reflection losses at the interface. A typical value of the refraction index is 1.000 for air, 1.526 for glass, and 1.33 for water.

Expressions for perpendicular and parallel components of radiation for smooth surfaces were derived by Fresnel as:

$$r_{\perp} = \frac{\sin^2(\theta_2 - \theta_1)}{\sin^2(\theta_2 + \theta_1)} \tag{2.45}$$

$$r_{\parallel} = \frac{\tan^2(\theta_2 - \theta_1)}{\tan^2(\theta_2 + \theta_1)} \tag{2.46}$$

Equation (2.45) represents the perpendicular component of unpolarized radiation and Eq. (2.46) represents the parallel one. It should be noted that *parallel* and *perpendicular* refer to the plane defined by the incident beam and the surface normal.

Properties are evaluated by calculating the average of these two components as:

$$r = \frac{1}{2}(r_{\perp} + r_{\parallel}) \tag{2.47}$$

For normal incidence, both angles are 0 and Eq. (2.47) can be combined with Eq. (2.44) to yield:

$$r_{(0)} = \left(\frac{n_1 - n_2}{n_1 + n_2}\right)^2 \tag{2.48}$$

If one medium is air ($n = 1.0$), then Eq. (2.48) becomes:

$$r_{(0)} = \left(\frac{n - 1}{n + 1}\right)^2 \tag{2.49}$$

Similarly, the transmittance, τ_r (subscript r indicates that only reflection losses are considered), can be calculated from the average transmittance of the two components as follows:

$$\tau_r = \frac{1}{2}\left(\frac{1 - r_{\parallel}}{1 + r_{\parallel}} + \frac{1 - r_{\perp}}{1 + r_{\perp}}\right) \tag{2.50a}$$

For a glazing system of N covers of the same material, it can be proven that:

$$\tau_r = \frac{1}{2}\left(\frac{1 - r_{\parallel}}{1 + (2N - 1)r_{\parallel}} + \frac{1 - r_{\perp}}{1 + (2N - 1)r_{\perp}}\right) \tag{2.50b}$$

The transmittance, τ_α (subscript α indicates that only absorption losses are considered), can be calculated from:

$$\tau_\alpha = e^{\left(-\frac{KL}{\cos\theta_2}\right)} \tag{2.51}$$

where K is the extinction coefficient, which can vary from 4m^{-1} (for high-quality glass) to 32m^{-1} (for low-quality glass), and L is the thickness of the glass cover.

The transmittance, reflectance, and absorptance of a single cover (by considering both reflection and absorption losses) are given by the following expressions. These expressions are for the perpendicular components of polarization, although the same relations can be used for the parallel components:

$$\tau_{\perp} = \frac{\tau_{\alpha}(1-r_{\perp})^2}{1-(r_{\perp}\tau_{\alpha})^2} = \tau_{\alpha}\frac{1-r_{\perp}}{1+r_{\perp}}\left(\frac{1-r_{\perp}^2}{1-(r_{\perp}\tau_{\alpha})^2}\right) \tag{2.52a}$$

$$\rho_{\perp} = r_{\perp} + \frac{(1-r_{\perp})^2\tau_{\alpha}^2 r_{\perp}}{1-(r_{\perp}\tau_{\alpha})^2} = r_{\perp}(1+\tau_{\alpha}\tau_{\perp}) \tag{2.52b}$$

$$\alpha_{\perp} = (1-\tau_{\alpha})\left(\frac{1-r_{\perp}}{1-r_{\perp}\tau_{\alpha}}\right) \tag{2.52c}$$

Since, for practical collector covers, τ_{α} is seldom less than 0.9 and r is of the order of 0.1, the transmittance of a single cover becomes:

$$\tau \cong \tau_{\alpha}\tau_{\mathrm{r}} \tag{2.53}$$

The absorptance of a cover can be approximated by neglecting the last term of Eq. (2.52c):

$$\alpha \cong 1-\tau_{\alpha} \tag{2.54}$$

and the reflectance of a single cover could be found (keeping in mind that $\rho = 1-\alpha-\tau$) as:

$$\rho \cong \tau_{\alpha}(1-\tau_{\mathrm{r}}) = \tau_{\alpha}-\tau \tag{2.55}$$

For a two-cover system of not necessarily same materials, the following equation can be obtained (subscript 1 refers to the outer cover and 2 to the inner one):

$$\tau = \frac{1}{2}\left[\left(\frac{\tau_1\tau_2}{1-\rho_1\rho_2}\right)_{\perp} + \left(\frac{\tau_1\tau_2}{1-\rho_1\rho_2}\right)_{||}\right] = \frac{1}{2}(\tau_{\perp}+\tau_{||}) \tag{2.56}$$

$$\rho = \frac{1}{2}\left[\left(\rho_1 + \frac{\tau\rho_2\tau_1}{\tau_2}\right)_{\perp} + \left(\rho_1 + \frac{\tau\rho_2\tau_1}{\tau_2}\right)_{||}\right] = \frac{1}{2}(\rho_{\perp}+\rho_{||}) \tag{2.57}$$

EXAMPLE 2.13

A solar energy collector uses a single glass cover with a thickness of 4 mm. In the visible solar range, the refraction index of glass, n, is 1.526 and its extinction coefficient K is $32\mathrm{m}^{-1}$. Calculate the reflectivity, transmissivity, and absorptivity of the glass sheet for the angle of incidence of 60° and at normal incidence (0°).

Solution

Angle of incidence $= 60^\circ$

From Eq. (2.44), the refraction angle θ_2 is calculated as:

$$\theta_2 = \sin^{-1}\left(\frac{\sin\theta_1}{n}\right) = \sin^{-1}\left(\frac{\sin(60)}{1.526}\right) = 34.6^\circ$$

From Eq. (2.51), the transmittance can be obtained as:

$$\tau_\alpha = e^{\left(-\frac{KL}{\cos(\theta_2)}\right)} = e^{\left(-\frac{32(0.004)}{\cos(34.6)}\right)} = 0.856$$

From Eqs (2.45) and (2.46),

$$r_\perp = \frac{\sin^2(\theta_2-\theta_1)}{\sin^2(\theta_2+\theta_1)} = \frac{\sin^2(34.6-60)}{\sin^2(34.6+60)} = 0.185$$

$$r_\parallel = \frac{\tan^2(\theta_2-\theta_1)}{\tan^2(\theta_2+\theta_1)} = \frac{\tan^2(34.6-60)}{\tan^2(34.6+60)} = 0.001$$

From Eqs (2.52a)–(2.52c), we have:

$$\tau = \frac{\tau_\alpha}{2}\left\{\frac{1-r_\perp}{1+r_\perp}\left[\frac{1-r_\perp^2}{1-(r_\perp\tau_\alpha)^2}\right] + \frac{1-r_\parallel}{1+r_\parallel}\left[\frac{1-r_\parallel^2}{1-(r_\parallel\tau_\alpha)^2}\right]\right\} = \frac{\tau_\alpha}{2}\left[\tau_\perp + \tau_\parallel\right]$$

$$= \frac{0.856}{2}\left\{\frac{1-0.185}{1+0.185}\left[\frac{1-0.185^2}{1-(0.185\times 0.856)^2}\right] + \frac{1-0.001}{1+0.001}\left[\frac{1-0.001^2}{1-(0.001\times 0.856)^2}\right]\right\}$$

$$= 0.428(0.681+0.998) = 0.719$$

$$\rho = \frac{1}{2}\left[r_\perp(1+\tau_\alpha\tau_\perp) + r_\parallel(1+\tau_\alpha\tau_\parallel)\right]$$

$$= 0.5[0.185(1+0.856\times 0.681) + 0.001(1+0.856\times 0.998)] = 0.147$$

$$\alpha = \frac{(1-\tau_\alpha)}{2}\left[\left(\frac{1-r_\perp}{1-r_\perp\tau_\alpha}\right) + \left(\frac{1-r_\parallel}{1-r_\parallel\tau_\alpha}\right)\right]$$

$$= \frac{(1-0.856)}{2}\left(\frac{1-0.185}{1-0.185\times 0.856} + \frac{1-0.001}{1-0.001\times 0.856}\right) = 0.142$$

Normal incidence

At normal incidence, $\theta_1 = 0°$ and $\theta_2 = 0°$. In this case, τ_α is equal to 0.880. There is no polarization at normal incidence; therefore, from Eq. (2.49),

$$r_{(0)} = r_\perp = r_\parallel = \left(\frac{n-1}{n+1}\right)^2 = \left(\frac{1.526-1}{1.526+1}\right)^2 = 0.043$$

From Eqs (2.52a)–(2.52c), we have:

$$\tau = \tau_\alpha \frac{1-r_{(0)}}{1+r_{(0)}}\left[\frac{1-r_{(0)}^2}{1-(r_{(0)}\tau_\alpha)^2}\right] = 0.880\left\{\frac{1-0.043}{1+0.043}\left[\frac{1-0.043^2}{1-(0.043\times 0.880)^2}\right]\right\} = 0.807$$

$$\rho = r_{(0)}(1+\tau_\alpha\tau_{(0)}) = 0.043(1+0.880\times 0.807) = 0.074$$

$$\alpha = (1-\tau_\alpha)\left(\frac{1-r_{(0)}}{1-r_{(0)}\tau_\alpha}\right) = (1-0.880)\left(\frac{1-0.043}{1-0.043\times 0.880}\right) = 0.119$$

2.3.4 Radiation exchange between surfaces

When studying the radiant energy exchanged between two surfaces separated by a non-absorbing medium, one should consider not only the temperature of the surfaces and their characteristics but also their geometric orientation with respect to each other. The effects of the geometry of radiant energy exchange can be analyzed conveniently by defining the term *view factor*, F_{12}, to be the fraction of radiation leaving surface A_1 that reaches surface A_2. If both surfaces are black, the radiation leaving surface A_1 and arriving at surface A_2 is $E_{b1}A_1F_{12}$, and the radiation leaving surface A_2 and arriving at surface A_1 is $E_{b2}A_2F_{21}$. If both surfaces are black and absorb all incident radiation, the net radiation exchange is given by:

$$Q_{12} = E_{b1}A_1F_{12} - E_{b2}A_2F_{21} \tag{2.58}$$

If both surfaces are of the same temperature, $E_{b1} = E_{b2}$ and $Q_{12} = 0$. Therefore,

$$A_1F_{12} = A_2F_{21} \tag{2.59}$$

It should be noted that Eq. (2.59) is strictly geometric in nature and valid for all diffuse emitters, irrespective of their temperatures. Therefore, the net radiation exchange between two black surfaces is given by:

$$Q_{12} = A_1F_{12}(E_{b1} - E_{b2}) = A_2F_{21}(E_{b1} - E_{b2}) \tag{2.60}$$

From Eq. (2.36a), $E_b = \sigma T^4$, Eq. (2.60) can be written as:

$$Q_{12} = A_1F_{12}\sigma(T_1^4 - T_2^4) = A_2F_{21}\sigma(T_1^4 - T_2^4) \tag{2.61}$$

where T_1 and T_2 are the temperatures of surfaces A_1 and A_2, respectively. As the term $(E_{b1} - E_{b2})$ in Eq. (2.60) is the energy potential difference that causes the transfer of heat, in a network of electric circuit analogy, the term $1/A_1F_{12} = 1/A_2F_{21}$ represents the resistance due to the geometric configuration of the two surfaces.

When surfaces other than black are involved in radiation exchange, the situation is much more complex, because multiple reflections from each surface must be taken into consideration. For the simple case of opaque gray surfaces, for which $\varepsilon = \alpha$, the reflectivity $\rho = 1 - \alpha = 1 - \varepsilon$. From Eq. (2.42), the radiosity of each surface is given by:

$$J = \varepsilon E_b + \rho H = \varepsilon E_b + (1 - \varepsilon)H \tag{2.62}$$

The net radiant energy leaving the surface is the difference between the radiosity, J, leaving the surface and the irradiation, H, incident on the surface; that is,

$$Q = A(J - H) \tag{2.63}$$

Combining Eqs (2.62) and (2.63) and eliminating irradiation H results in:

$$Q = A\left(J - \frac{J - \varepsilon E_b}{1 - \varepsilon}\right) = \frac{A\varepsilon}{1 - \varepsilon}(E_b - J) = \frac{(E_b - J)}{R} \tag{2.64}$$

Therefore, the net radiant energy leaving a gray surface can be regarded as the current in an equivalent electrical network when a potential difference $(E_b - J)$ is overcome across a resistance $R = (1 - \varepsilon)/A\varepsilon$. This resistance, called *surface resistance*, is due to the imperfection of the surface as an emitter and absorber of radiation as compared with a black surface.

By considering the radiant energy exchange between two gray surfaces, A_1 and A_2, the radiation leaving surface A_1 and arriving at surface A_2 is $J_1A_1F_{12}$, where J is the radiosity, given by Eq. (2.42). Similarly, the radiation leaving surface A_2 and arriving surface A_1 is $J_2A_2F_{21}$. The net radiation exchange between the two surfaces is given by:

$$Q_{12} = J_1A_1F_{12} - J_2A_2F_{21} = A_1F_{12}(J_1 - J_2) = A_2F_{21}(J_1 - J_2) \tag{2.65}$$

Therefore, due to the geometric orientation that applies between the two potentials, J_1 and J_2, when two gray surfaces exchange radiant energy, there is a resistance, called *space resistance*, $R = 1/A_1F_{12} = 1/A_2F_{21}$.

An equivalent electric network for two the gray surfaces is illustrated in Figure 2.24. By combining the surface resistance, $(1 - \varepsilon)/A\varepsilon$ for each surface and the space (or geometric) resistance,

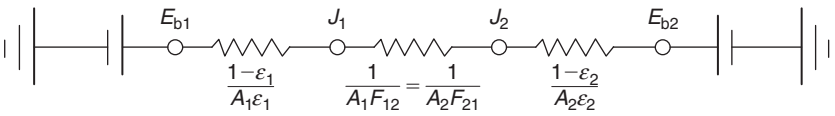

FIGURE 2.24

Equivalent electrical network for radiation exchange between two gray surfaces.

$1/A_1F_{12} = 1/A_2F_{21}$, between the surfaces, as shown in Figure 2.24, the net rate of radiation exchange between the two surfaces is equal to the overall potential difference divided by the sum of resistances, given by:

$$Q_{12} = \frac{E_{b1} - E_{b2}}{\left[\frac{(1-\varepsilon_1)}{A_1\varepsilon_1}\right] + \frac{1}{A_1F_{12}} + \left[\frac{(1-\varepsilon_2)}{A_2\varepsilon_2}\right]} = \frac{\sigma\left(T_1^4 - T_2^4\right)}{\left[\frac{(1-\varepsilon_1)}{A_1\varepsilon_1}\right] + \frac{1}{A_1F_{12}} + \left[\frac{(1-\varepsilon_2)}{A_2\varepsilon_2}\right]} \tag{2.66}$$

In solar energy applications, the following geometric orientations between two surfaces are of particular interest.

A. For two infinite parallel surfaces, $A_1 = A_2 = A$ and $F_{12} = 1$, Eq. (2.66) becomes:

$$Q_{12} = \frac{A\sigma\left(T_1^4 - T_2^4\right)}{(1/\varepsilon_1) + (1/\varepsilon_2) - 1} \tag{2.67}$$

B. For two concentric cylinders, $F_{12} = 1$ and Eq. (2.66) becomes:

$$Q_{12} = \frac{A_1\sigma\left(T_1^4 - T_2^4\right)}{(1/\varepsilon_1) + (A_1/A_2)[(1/\varepsilon_2) - 1]} \tag{2.68}$$

C. For a small convex surface, A_1, completely enclosed by a very large concave surface, A_2, $A_1 << A_2$ and $F_{12} = 1$, then Eq. (2.66) becomes:

$$Q_{12} = A_1\varepsilon_1\sigma\left(T_1^4 - T_2^4\right) \tag{2.69}$$

The last equation also applies for a flat-plate collector cover radiating to the surroundings, whereas case B applies in the analysis of a parabolic trough collector receiver where the receiver pipe is enclosed in a glass cylinder.

As can be seen from Eqs (2.67)–(2.69), the rate of radiative heat transfer between surfaces depends on the difference of the fourth power of the surface temperatures. In many engineering calculations, however, the heat transfer equations are linearized in terms of the differences of temperatures to the first power. For this purpose, the following mathematical identity is used:

$$T_1^4 - T_2^4 = \left(T_1^2 - T_2^2\right)\left(T_1^2 + T_2^2\right) = (T_1 - T_2)(T_1 + T_2)\left(T_1^2 + T_2^2\right) \tag{2.70}$$

Therefore, Eq. (2.66) can be written as:

$$Q_{12} = A_1h_r(T_1 - T_2) \tag{2.71}$$

with the radiation heat transfer coefficient, h_r, defined as:

$$h_r = \frac{\sigma(T_1 + T_2)\left(T_1^2 + T_2^2\right)}{\frac{1-\varepsilon_1}{\varepsilon_1} + \frac{1}{F_{12}} + \frac{A_1}{A_2}\left(\frac{1-\varepsilon_2}{\varepsilon_2}\right)} \tag{2.72}$$

For the special cases mentioned previously, the expressions for h_r are as follows:

Case A:

$$h_r = \frac{\sigma(T_1 + T_2)\left(T_1^2 + T_2^2\right)}{\dfrac{1}{\varepsilon_1} + \dfrac{1}{\varepsilon_2} - 1} \tag{2.73}$$

Case B:

$$h_r = \frac{\sigma(T_1 + T_2)\left(T_1^2 + T_2^2\right)}{\dfrac{1}{\varepsilon_1} + \dfrac{A_1}{A_2}\left(\dfrac{1}{\varepsilon_2} - 1\right)} \tag{2.74}$$

Case C:

$$h_r = \varepsilon_1 \sigma(T_1 + T_2)\left(T_1^2 + T_2^2\right) \tag{2.75}$$

It should be noted that the use of these linearized radiation equations in terms of h_r is very convenient when the equivalent network method is used to analyze problems involving conduction and/or convection in addition to radiation. The radiation heat transfer coefficient, h_r, is treated similarly to the convection heat transfer coefficient, h_c, in an electric equivalent circuit. In such a case, a combined heat transfer coefficient can be used, given by:

$$h_{cr} = h_c + h_r \tag{2.76}$$

In this equation, it is assumed that the linear temperature difference between the ambient fluid and the walls of the enclosure and the surface and the enclosure substances are at the same temperature.

EXAMPLE 2.14

The glass of a 1×2 m flat-plate solar collector is at a temperature of 80 °C and has an emissivity of 0.90. The environment is at a temperature of 15 °C. Calculate the convection and radiation heat losses if the convection heat transfer coefficient is 5.1 W/m^{2}K.

Solution

In the following analysis, the glass cover is denoted by subscript 1 and the environment by 2. The radiation heat transfer coefficient is given by Eq. (2.75):

$$\begin{aligned} h_r &= \varepsilon_1 \sigma(T_1 + T_2)\left(T_1^2 + T_2^2\right) \\ &= 0.90 \times 5.67 \times 10^{-8}\left(353 + 288\right)\left(353^2 + 288^2\right) \\ &= 6.789 \text{ W/m}^2 \text{ K} \end{aligned}$$

Therefore, from Eq. (2.76),

$$h_{cr} = h_c + h_r = 5.1 + 6.789 = 11.889 \text{ W/m}^2 \text{ K}$$

Finally,

$$Q_{12} = A_1 h_{cr}(T_1 - T_2) = (1 \times 2)(11.889)(353 - 288) = 1545.6 \text{ W}$$

EXAMPLE 2.15

Two very large parallel plates are maintained at uniform temperatures of 900 K and 400 K. The emissivities of the two surfaces are 0.3 and 0.8, respectively. What is the radiation heat transfer between the two surfaces?

Solution

As the areas of the two surfaces are not given the estimation is given per unit surface area of the plates. As the two plates are very large and parallel, Eq. (2.67) apply, so:

$$\frac{Q_{12}}{A} = \frac{\sigma\left(T_1^4 - T_2^4\right)}{\left(\frac{1}{\varepsilon_1}\right) + \left(\frac{1}{\varepsilon_2}\right) - 1} = \frac{5.67 \times 10^{-8}\left(900^4 - 400^4\right)}{\frac{1}{0.3} + \frac{1}{0.8} - 1} = 9976.6 \text{ W/m}^2$$

EXAMPLE 2.16

Two very long concentric cylinders of diameters 30 and 50 cm are maintained at uniform temperatures of 850 K and 450 K. The emissivities of the two surfaces are 0.9 and 0.6, respectively. The space between the two cylinders is evacuated. What is the radiation heat transfer between the two cylinders per unit length of the cylinders?

Solution

For concentric cylinders Eq. (2.68) applies. Therefore,

$$Q_{12} = \frac{A_1\sigma\left(T_1^4 - T_2^4\right)}{\left(\frac{1}{\varepsilon_1}\right) + \left(\frac{A_1}{A_2}\right)\left(\frac{1-\varepsilon_2}{\varepsilon_2}\right)} = \frac{\pi \times 0.3 \times 1 \times 5.67 \times 10^{-8}\left(850^4 - 450^4\right)}{\frac{1}{0.9} + \left(\frac{30}{50}\right)\left(\frac{1-0.6}{0.6}\right)} = 17 \text{ kW}$$

2.3.5 Extraterrestrial solar radiation

The amount of solar energy per unit time, at the mean distance of the earth from the sun, received on a unit area of a surface normal to the sun (perpendicular to the direction of propagation of the radiation) outside the atmosphere is called the *solar constant*, G_{sc}. This quantity is difficult to measure from the surface of the earth because of the effect of the atmosphere. A method for the determination of the solar constant was first given in 1881 by Langley (Garg, 1982), who had given his name to the units of measurement as Langleys per minute (calories per square centimeter per minute). This was changed by the SI system to Watts per square meter (W/m^2).

When the sun is closest to the earth, on January 3, the solar heat on the outer edge of the earth's atmosphere is about 1400 W/m^2; and when the sun is farthest away, on July 4, it is about 1330 W/m^2.

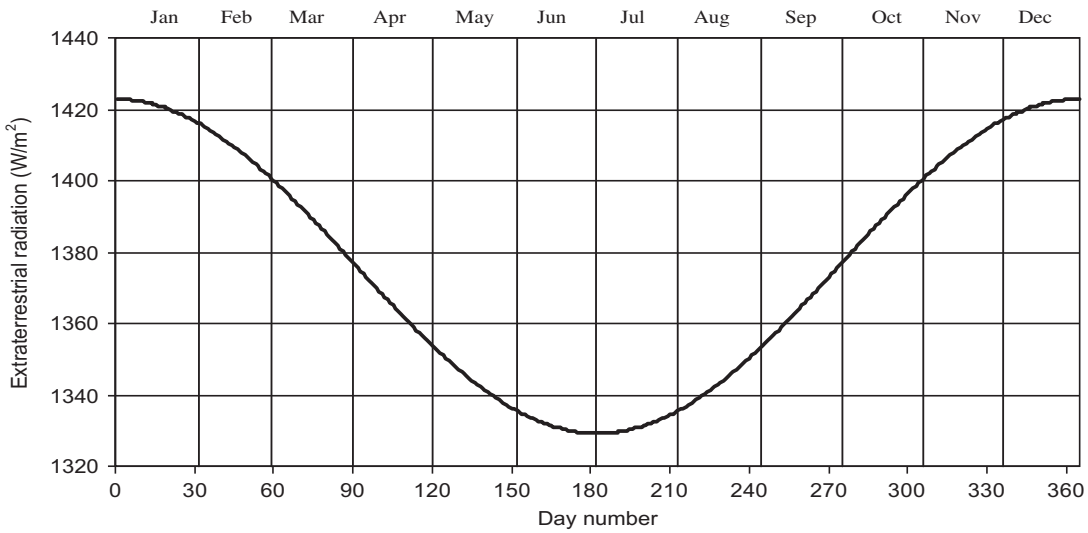

FIGURE 2.25

Variation of extraterrestrial solar radiation with the time of year.

Throughout the year, the extraterrestrial radiation measured on the plane normal to the radiation on the Nth day of the year, G_{on}, varies between these limits, as indicated in Figure 2.25, in the range of 3.3% and can be calculated by (Duffie and Beckman, 1991; Hsieh, 1986):

$$G_{on} = G_{sc}\left[1 + 0.033\cos\left(\frac{360N}{365}\right)\right] \tag{2.77}$$

where

G_{on} = extraterrestrial radiation measured on the plane normal to the radiation on the Nth day of the year (W/m^2).
G_{sc} = solar constant (W/m^2).

The latest value of G_{sc} is 1366.1 W/m^2. This was adopted in 2000 by the American Society for Testing and Materials (ASTM), which developed an AM0 reference spectrum (ASTM E-490). The ASTM E-490 Air Mass Zero solar spectral irradiance is based on data from satellites, space shuttle missions, high-altitude aircraft, rocket soundings, ground-based solar telescopes, and modeled spectral irradiance. The spectral distribution of extraterrestrial solar radiation at the mean sun–earth distance is shown in Figure 2.26. The spectrum curve of Figure 2.26 is based on a set of data included in ASTM E-490 (Solar Spectra, 2007).

When a surface is placed parallel to the ground, the rate of solar radiation, G_{oH}, incident on this extraterrestrial horizontal surface at a given time of the year is given by:

$$G_{oH} = G_{on}\cos(\Phi) = G_{sc}\left[1 + 0.033\cos\left(\frac{360N}{365}\right)\right][\cos(L)\cos(\delta)\cos(h) + \sin(L)\sin(\delta)] \tag{2.78}$$

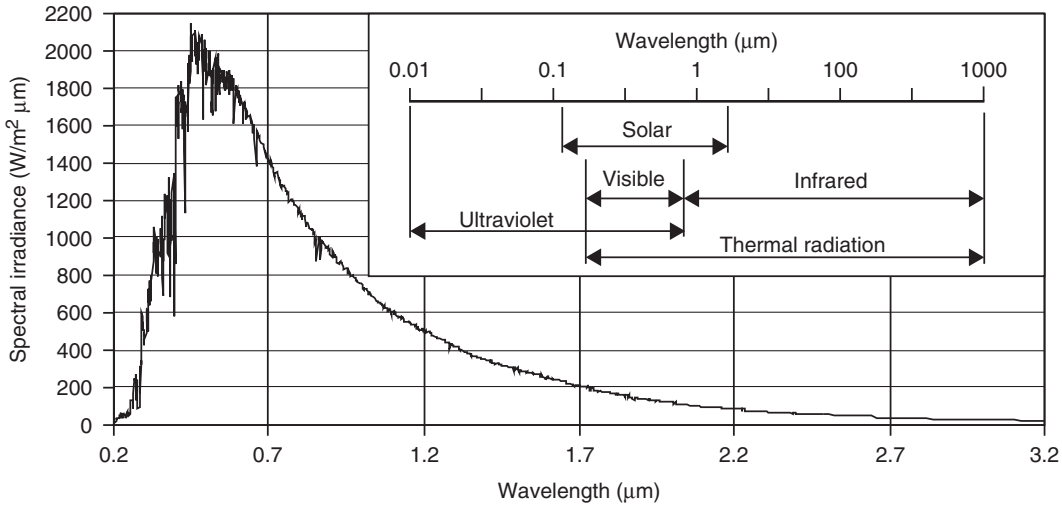

FIGURE 2.26

Standard curve giving a solar constant of 1366.1 W/m^2 and its position in the electromagnetic radiation spectrum.

The total radiation, H_o, incident on an extraterrestrial horizontal surface during a day can be obtained by the integration of Eq. (2.78) over a period from sunrise to sunset. The resulting equation is:

$$H_o = \frac{24 \times 3600 G_{sc}}{\pi}\left[1 + 0.033\cos\left(\frac{360N}{365}\right)\right] \times \left[\cos(L)\cos(\delta)\sin(h_{ss}) + \left(\frac{\pi h_{ss}}{180}\right)\sin(L)\sin(\delta)\right] \tag{2.79}$$

where h_{ss} is the sunset hour in degrees, obtained from Eq. (2.15). The units of Eq. (2.79) are joules per square meter (J/m^2).

To calculate the extraterrestrial radiation on a horizontal surface for an hour period, Eq. (2.78) is integrated between hour angles, h_1 and h_2 (h_2 is larger). Therefore,

$$I_o = \frac{12 \times 3600 G_{sc}}{\pi}\left[1 + 0.033\cos\left(\frac{360N}{365}\right)\right] \times \left\{\cos(L)\cos(\delta)\left[\sin(h_2) - \sin(h_1)\right] + \left[\frac{\pi(h_2 - h_1)}{180}\right]\sin(L)\sin(\delta)\right\} \tag{2.80}$$

It should be noted that the limits h_1 and h_2 may define a time period other than 1 h.

EXAMPLE 2.17

Determine the extraterrestrial normal radiation and the extraterrestrial radiation on a horizontal surface on March 10 at 2:00 pm solar time for 35°N latitude. Determine also the total solar radiation on the extraterrestrial horizontal surface for the day.

Solution

The declination on March 10 ($N = 69$) is calculated from Eq. (2.5):

$$\delta = 23.45 \sin\left[\frac{360}{365}(284 + 69)\right] = -4.8^\circ$$

The hour angle at 2:00 pm solar time is calculated from Eq. (2.8):

$$h = 0.25 \text{ (number of minutes from local solar noon)} = 0.25(120) = 30^\circ$$

The hour angle at sunset is calculated from Eq. (2.15):

$$h_{ss} = \cos^{-1}\left[-\tan(L)\tan(\delta)\right] = \cos^{-1}\left[-\tan(35)\tan(-4.8)\right] = 86.6^\circ$$

The extraterrestrial normal radiation is calculated from Eq. (2.77):

$$G_{on} = G_{sc}\left[1 + 0.033\cos\left(\frac{360N}{365}\right)\right] = 1366\left[1 + 0.033\cos\left(\frac{360 \times 69}{365}\right)\right] = 1383 \text{ W/m}^2$$

The extraterrestrial radiation on a horizontal surface is calculated from Eq. (2.78):

$$\begin{aligned} G_{oH} &= G_{on}\cos(\Phi) = G_{on}[\sin(L)\sin(\delta) + \cos(L)\cos(\delta)\cos(h)] \\ &= 1383\left[\sin(35)\sin(-4.8) + \cos(35)\cos(-4.8)\cos(30)\right] = 911 \text{ W/m}^2 \end{aligned}$$

The total radiation on the extraterrestrial horizontal surface is calculated from Eq. (2.79):

$$H_o = \frac{24 \times 3600 G_{sc}}{\pi}\left[1 + 0.033\cos\left(\frac{360N}{365}\right)\right]\left[\cos(L)\cos(\delta)\sin(h_{ss}) + \left(\frac{\pi h_{ss}}{180}\right)\sin(L)\sin(\delta)\right]$$

$$= \frac{24 \times 3600 \times 1383}{\pi}\left[\begin{array}{l}\cos(35)\cos(-4.8)\sin(86.6) \\ +\left(\frac{\pi \times 86.6}{180}\right)\sin(35)\sin(-4.8)\end{array}\right] = 28.23 \text{ MJ/m}^2$$

A list of definitions that includes those related to solar radiation is found in Appendix 2. The reader should familiarize himself or herself with the various terms and specifically with *irradiance*, which is the rate of radiant energy falling on a surface per unit area of the surface (units, watts per square meter [W/m^2] symbol, G), whereas *irradiation* is incident energy per unit area on a surface (units, joules per square meter [J/m^2]), obtained by integrating irradiance over a specified time interval. Specifically, for

solar irradiance this is called *insolation*. The symbols used in this book are H for insolation for a day and I for insolation for an hour. The appropriate subscripts used for G, H, and I are beam (B), diffuse (D), and ground-reflected (G) radiation.

2.3.6 Atmospheric attenuation

The solar heat reaching the earth's surface is reduced below G_{on} because a large part of it is scattered, reflected back out into space, and absorbed by the atmosphere. As a result of the atmospheric interaction with the solar radiation, a portion of the originally collimated rays becomes scattered or non-directional. Some of this scattered radiation reaches the earth's surface from the entire sky vault. This is called the *diffuse radiation*. The solar heat that comes directly through the atmosphere is termed *direct* or *beam radiation*. The insolation received by a surface on earth is the sum of diffuse radiation and the normal component of beam radiation. The solar heat at any point on earth depends on:

1. The ozone layer thickness
2. The distance traveled through the atmosphere to reach that point
3. The amount of haze in the air (dust particles, water vapor, etc.)
4. The extent of the cloud cover

The earth is surrounded by atmosphere that contains various gaseous constituents, suspended dust, and other minute solid and liquid particulate matter and clouds of various types. As the solar radiation travels through the earth's atmosphere, waves of very short length, such as X-rays and gamma rays, are absorbed in the ionosphere at extremely high altitude. The waves of relatively longer length, mostly in the ultraviolet range, are then absorbed by the layer of ozone (O_3), located about 15–40 km above the earth's surface. In the lower atmosphere, bands of solar radiation in the infrared range are absorbed by water vapor and carbon dioxide. In the long-wavelength region, since the extraterrestrial radiation is low and the H_2O and CO_2 absorption is strong, little solar energy reaches the ground.

Therefore, the solar radiation is depleted during its passage though the atmosphere before reaching the earth's surface. The reduction of intensity with increasing zenith angle of the sun is generally assumed to be directly proportional to the increase in air mass, an assumption that considers the atmosphere to be unstratified with regard to absorbing or scattering impurities.

The degree of attenuation of solar radiation traveling through the earth's atmosphere depends on the length of the path and the characteristics of the medium traversed. In solar radiation calculations, one standard *air mass* is defined as the length of the path traversed in reaching the sea level when the sun is at its zenith (the vertical at the point of observation). The air mass is related to the zenith angle, Φ (Figure 2.27), without considering the earth's curvature, by the equation:

$$m = \frac{AB}{BC} = \frac{1}{\cos(\Phi)} \tag{2.81}$$

Therefore, at sea level when the sun is directly overhead, that is, when $\Phi = 0^\circ$, $m = 1$ (air mass one); and when $\Phi = 60^\circ$, we get $m = 2$ (air mass two). Similarly, the solar radiation outside the earth's atmosphere is at air mass zero. The graph of direct normal irradiance (solar spectrum) at ground level for air mass 1.5 is shown in Appendix 4.

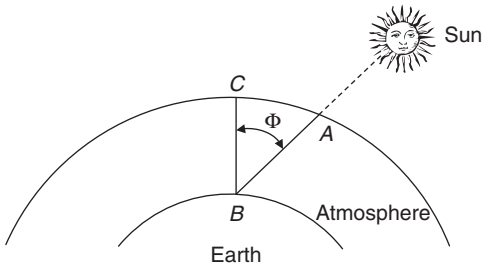

FIGURE 2.27

Air mass definition.

2.3.7 Terrestrial irradiation

A solar system frequently needs to be judged on its long-term performance. Therefore, knowledge of long-term monthly average daily insolation data for the locality under consideration is required. Daily mean total solar radiation (beam plus diffuse) incident on a horizontal surface for each month of the year is available from various sources, such as radiation maps or a country's meteorological service (see Section 2.4). In these sources, data, such as 24 h average temperature, monthly average daily radiation on a horizontal surface $\overline{\mathrm{H}}$ (MJ/m^2 day), and monthly average clearness index, $\overline{K}_\mathrm{T}$, are given together with other parameters, which are not of interest here.[2] The monthly average clearness index, $\overline{K}_\mathrm{T}$, is defined as:

$$\overline{K}_\mathrm{T} = \frac{\overline{H}}{\overline{H}_\mathrm{o}} \tag{2.82a}$$

where

$\overline{H}$ = monthly average daily total radiation on a terrestrial horizontal surface (MJ/m^2 day).
$\overline{H}_\mathrm{o}$ = monthly average daily total radiation on an extraterrestrial horizontal surface (MJ/m^2 day).

The bar over the symbols signifies a long-term average. The value of $\overline{H}_\mathrm{o}$ can be calculated from Eq. (2.79) by choosing a particular day of the year in the given month for which the daily total extraterrestrial insolation is estimated to be the same as the monthly mean value. Table 2.5 gives the values of $\overline{H}_\mathrm{o}$ for each month as a function of latitude, together with the recommended dates of each month that would give the mean daily values of $\overline{H}_\mathrm{o}$. The day number and the declination of the day for the recommended dates are shown in Table 2.1. For the same days, the monthly average daily extraterrestrial insolation on a horizontal surface for various months in kilowatt hours per square meter (kWh/m^2 day) for latitudes -60° to $+60^\circ$ is also shown graphically in Figure A3.5 in Appendix 3, from which we can easily interpolate.

Further to Eq. (2.82a) the daily clearness index $K_\mathrm{T,}$ can be defined as the ratio of the radiation for a particular day to the extraterrestrial radiation for that day given by:

$$K_\mathrm{T} = \frac{H}{H_\mathrm{o}} \tag{2.82b}$$

[2]Meteorological data for various locations are shown in Appendix 7.

Table 2.5 Monthly Average Daily Extraterrestrial Insolation on Horizontal Surface (MJ/m^2)

Latitude	Jan 17	Feb 16	Mar 16	Apr 15	May 15	June 11	July 17	Aug 16	Sept 15	Oct 15	Nov 14	Dec 10
60°S	41.1	31.9	21.2	10.9	4.4	2.1	3.1	7.8	16.7	28.1	38.4	43.6
55°S	41.7	33.7	23.8	13.8	7.1	4.5	5.6	10.7	19.5	30.2	39.4	43.9
50°S	42.4	35.3	26.3	16.8	10.0	7.2	8.4	13.6	22.2	32.1	40.3	44.2
45°S	42.9	36.8	28.6	19.6	12.9	10.0	11.2	16.5	24.7	33.8	41.1	44.4
40°S	43.1	37.9	30.7	22.3	15.8	12.9	14.1	19.3	27.1	35.3	41.6	44.4
35°S	43.2	38.8	32.5	24.8	18.6	15.8	17.0	22.0	29.2	36.5	41.9	44.2
30°S	43.0	39.5	34.1	27.2	21.4	18.7	19.8	24.5	31.1	37.5	41.9	43.7
25°S	42.5	39.9	35.4	29.4	24.1	21.5	22.5	26.9	32.8	38.1	41.6	43.0
20°S	41.5	39.9	36.5	31.3	26.6	24.2	25.1	29.1	34.2	38.5	41.1	42.0
15°S	40.8	39.7	37.2	33.1	28.9	26.8	27.6	31.1	35.4	38.7	40.3	40.8
10°S	39.5	39.3	37.7	34.6	31.1	29.2	29.9	32.8	36.3	38.5	39.3	39.3
5°S	38.0	38.5	38.0	35.8	33.0	31.4	32.0	34.4	36.9	38.1	37.9	37.6
0	36.2	37.4	37.9	36.8	34.8	33.5	33.9	35.7	37.2	37.3	36.4	35.6
5°N	34.2	36.1	37.5	37.5	36.3	35.3	35.6	36.7	37.3	36.3	34.5	33.5
10°N	32.0	34.6	36.9	37.9	37.5	37.0	37.1	37.5	37.0	35.1	32.5	31.1
15°N	29.5	32.7	35.9	38.0	38.5	38.4	38.3	38.0	36.5	33.5	30.2	28.5
20°N	26.9	30.7	34.7	37.9	39.3	39.5	39.3	38.2	35.7	31.8	27.7	25.7
25°N	24.1	28.4	33.3	37.5	39.8	40.4	40.0	38.2	34.7	29.8	25.1	22.9
30°N	21.3	26.0	31.6	36.8	40.0	41.1	40.4	37.9	33.4	27.5	22.3	19.9
35°N	18.3	23.3	29.6	35.8	39.9	41.5	40.6	37.3	31.8	25.1	19.4	16.8
40°N	15.2	20.5	27.4	34.6	39.7	41.7	40.6	36.5	30.0	22.5	16.4	13.7
45°N	12.1	17.6	25.0	33.1	39.2	41.7	40.4	35.4	27.9	19.8	13.4	10.7
50°N	9.1	14.6	22.5	31.4	38.4	41.5	40.0	34.1	25.7	16.9	10.4	7.7
55°N	6.1	11.6	19.7	29.5	37.6	41.3	39.4	32.7	23.2	13.9	7.4	4.8
60°N	3.4	8.5	16.8	27.4	36.6	41.0	38.8	31.0	20.6	10.9	4.5	2.3

Similarly, an hourly clearness index k_T, can be defined given by:

$$k_T = \frac{I}{I_o} \tag{2.82c}$$

In all these equations the values of $\overline{H}$, H, and I can be obtained from measurements of total solar radiation on horizontal using a pyranometer (see section 2.3.9).

To predict the performance of a solar system, hourly values of radiation are required. Because in most cases these types of data are not available, long-term average daily radiation data can be utilized to estimate long-term average radiation distribution. For this purpose, empirical correlations are usually used. Two such frequently used correlations are the Liu and Jordan (1977) correlation for the diffuse radiation and the Collares-Pereira and Rabl (1979) correlation for the total radiation.

According to the Liu and Jordan (1977) correlation,

$$r_d = \left(\frac{\pi}{24}\right)\frac{\cos(h) - \cos(h_{ss})}{\sin(h_{ss}) - \left(\frac{2\pi h_{ss}}{360}\right)\cos(h_{ss})} \tag{2.83}$$

where

r_d = ratio of hourly diffuse radiation to daily diffuse radiation (=I_D/H_D).
h_{ss} = sunset hour angle (degrees).
h = hour angle in degrees at the midpoint of each hour.

According to the Collares-Pereira and Rabl (1979) correlation,

$$r = \frac{\pi}{24}[\alpha + \beta\cos(h)]\frac{\cos(h) - \cos(h_{ss})}{\sin(h_{ss}) - \left(\frac{2\pi h_{ss}}{360}\right)\cos(h_{ss})} \tag{2.84a}$$

where

r = ratio of hourly total radiation to daily total radiation (=I/H).

$$\alpha = 0.409 + 0.5016\sin(h_{ss} - 60) \tag{2.84b}$$

$$\beta = 0.6609 - 0.4767\sin(h_{ss} - 60) \tag{2.84c}$$

EXAMPLE 2.18

Given the following empirical equation,

$$\frac{\overline{H}_D}{\overline{H}} = 1.390 - 4.027\overline{K}_T + 5.531\overline{K}_T^2 - 3.108\overline{K}_T^3$$

where $\overline{H}_D$ is the monthly average daily diffuse radiation on horizontal surface—see Eq. (2.105a)—estimate the average total radiation and the average diffuse radiation between 11:00 am and 12:00

pm solar time in the month of July on a horizontal surface located at 35°N latitude. The monthly average daily total radiation on a horizontal surface, $\overline{H}$, in July at the surface location is 23.14 MJ/m^2 day.

Solution

From Table 2.5 at 35° N latitude for July, $\overline{H}_o = 40.6$ MJ/m^2. Therefore,

$$\overline{K}_T = \frac{\overline{H}}{\overline{H}_o} = \frac{23.14}{40.6} = 0.570$$

Therefore,

$$\frac{\overline{H}_D}{\overline{H}} = 1.390 - 4.027(0.57) + 5.531(0.57)^2 - 3.108(0.57)^3 = 0.316$$

and

$$\overline{H}_D = 0.316\overline{H} = 0.316(23.14) = 7.31 \text{ MJ/m}^2 \text{ day}$$

From Table 2.5, the recommended average day for the month is July 17 ($N = 198$). The solar declination is calculated from Eq. (2.5) as:

$$\delta = 23.45 \sin\left[\frac{360}{365}(284 + N)\right] = 23.45 \sin\left[\frac{360}{365}(284 + 198)\right] = 21.2°$$

The sunset hour angle is calculated from Eq. (2.15) as:

$$\cos(h_{ss}) = -\tan(L)\tan(\delta) \rightarrow h_{ss} = \cos^{-1}\left[-\tan(35)\tan(21.2)\right] = 106°$$

The middle point of the hour from 11:00 am to 12:00 pm is 0.5 h from solar noon, or hour angle is −7.5°. Therefore, from Eqs. (2.84b), (2.84c) and (2.84a), we have:

$$\alpha = 0.409 + 0.5016 \sin(h_{ss} - 60) = 0.409 + 0.5016 \sin(106 - 60) = 0.77$$

$$\beta = 0.6609 - 0.4767 \sin(h_{ss} - 60) = 0.6609 - 0.4767 \sin(106 - 60) = 0.318$$

$$r = \frac{\pi}{24}(\alpha + \beta \cos(h)) \frac{\cos(h) - \cos(h_{ss})}{\sin(h_{ss}) - \left(\frac{2\pi h_{ss}}{360}\right)\cos(h_{ss})}$$

$$= \frac{\pi}{24}(0.77 + 0.318 \cos(-7.5)) \frac{\cos(-7.5) - \cos(106)}{\sin(106) - \left[\frac{2\pi(106)}{360}\right]\cos(106)} = 0.123$$

From Eq. (2.83), we have:

$$r_d = \left(\frac{\pi}{24}\right) \frac{\cos(h) - \cos(h_{ss})}{\sin(h_{ss}) - \left(\frac{2\pi h_{ss}}{360}\right)\cos(h_{ss})} = \left(\frac{\pi}{24}\right) \frac{\cos(-7.5) - \cos(106)}{\sin(106) - \left[\frac{2\pi(106)}{360}\right]\cos(106)} = 0.113$$

Finally,

$$\text{Average hourly total radiation} = 0.123(23.14) = 2.85 \text{ MJ/m}^2 \text{ or } 2850 \text{ kJ/m}^2$$

$$\text{Average hourly diffuse radiation} = 0.113(7.31) = 0.826 \text{ MJ/m}^2 \text{ or } 826 \text{ kJ/m}^2$$

2.3.8 Total radiation on tilted surfaces

Usually, collectors are not installed horizontally but at an angle to increase the amount of radiation intercepted and reduce reflection and cosine losses. Therefore, system designers need data about solar radiation on such titled surfaces; measured or estimated radiation data, however, are mostly available either for normal incidence or for horizontal surfaces. Therefore, there is a need to convert these data to radiation on tilted surfaces.

The amount of insolation on a terrestrial surface at a given location for a given time depends on the orientation and slope of the surface.

A flat surface absorbs beam (G_{Bt}), diffuse (G_{Dt}), and ground-reflected (G_{Gt}) solar radiation; that is,

$$G_t = G_{Bt} + G_{Dt} + G_{Gt} \tag{2.85}$$

As shown in Figure 2.28, the beam radiation on a tilted surface is:

$$G_{Bt} = G_{Bn}\cos(\theta) \tag{2.86}$$

and on a horizontal surface,

$$G_B = G_{Bn}\cos(\Phi) \tag{2.87}$$

where

G_{Bt} = beam radiation on a tilted surface (W/m^2).
G_B = beam radiation on a horizontal surface (W/m^2).

It follows that,

$$R_B = \frac{G_{Bt}}{G_B} = \frac{\cos(\theta)}{\cos(\Phi)} \tag{2.88}$$

where R_B is called the *beam radiation tilt factor*. The term $\cos(\theta)$ can be calculated from Eq. (2.86) and $\cos(\Phi)$ from Eq. (2.87). So the beam radiation component for any surface is:

$$G_{Bt} = G_B R_B \tag{2.89}$$

In Eq. (2.88), the zenith angle can be calculated from Eq. (2.12) and the incident angle θ can be calculated from Eq. (2.18) or, for the specific case of a south-facing fixed surface, from Eq. (2.20). Therefore, for a fixed surface facing south with tilt angle β, Eq. (2.88) becomes:

$$R_B = \frac{\cos(\theta)}{\cos(\Phi)} = \frac{\sin(L-\beta)\sin(\delta) + \cos(L-\beta)\cos(\delta)\cos(h)}{\sin(L)\sin(\delta) + \cos(L)\cos(\delta)\cos(h)} \tag{2.90a}$$

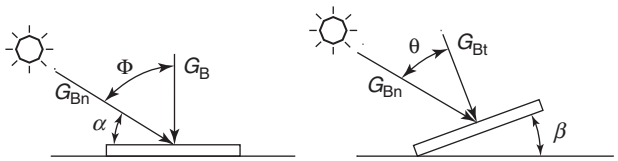

FIGURE 2.28

Beam radiation on horizontal and tilted surfaces.

Equation (2.88) also can be applied to surfaces other than fixed, in which case the appropriate equation for $\cos(\theta)$, as given in Section 2.2.1, can be used. For example, for a surface rotated continuously about a horizontal east–west axis, from Eq. (2.26a), the ratio of beam radiation on the surface to that on a horizontal surface at any time is given by:

$$R_B = \frac{\sqrt{1 - \cos^2(\delta)\sin^2(h)}}{\sin(L)\sin(\delta) + \cos(L)\cos(\delta)\cos(h)} \tag{2.90b}$$

EXAMPLE 2.19

Estimate the beam radiation tilt factor for a surface located at 35°N latitude and tilted 45° at 2:00 pm solar time on March 10. If the beam radiation at normal incidence is 900 W/m^2, estimate the beam radiation on the tilted surface.

Solution

From Example 2.17, $\delta = -4.8°$ and $h = 30°$. The beam radiation tilt factor is calculated from Eq. (2.90a) as:

$$R_B = \frac{\sin(L-\beta)\sin(\delta) + \cos(L-\beta)\cos(\delta)\cos(h)}{\sin(L)\sin(\delta) + \cos(L)\cos(\delta)\cos(h)}$$
$$= \frac{\sin(35-45)\sin(-4.8) + \cos(35-45)\cos(-4.8)\cos(30)}{\sin(35)\sin(-4.8) + \cos(35)\cos(-4.8)\cos(30)} = 1.312$$

Therefore, the beam radiation on the tilted surface is calculated from Eq. (2.89) as:

$$G_{Bt} = G_B R_B = 900(1.312) = 1181 \text{ W/m}^2$$

Isotropic sky model

Many models give the solar radiation on a tilted surface. The first one is the isotropic sky model developed originally by Hottel and Woertz (1942) and refined by Liu and Jordan (1960). According to this model, radiation is calculated as follows.

Diffuse radiation on a horizontal surface,

$$G_D = 2\int_0^{\pi/2} G_R \cos(\Phi)\, d\Phi = 2G_R \tag{2.91}$$

where

G_R = diffuse sky radiance (W/m^2 rad).

Diffuse radiation on a tilted surface,

$$G_{Dt} = \int_0^{\pi/2-\beta} G_R \cos(\Phi)\, d\Phi + \int_0^{\pi/2} G_R \cos(\Phi)\, d\Phi \tag{2.92}$$

where β is the surface tilt angle as shown in Figure 2.28.

From Eq. (2.91), the second term of Eq. (2.92) becomes $G_R = G_D/2$. Therefore, Eq. (2.92) becomes:

$$G_{Dt} = \frac{G_D}{2}\int_0^{\pi/2-\beta} \cos(\Phi)\, d\Phi + \frac{G_D}{2} = \frac{G_D}{2}\left[\sin\left(\frac{\pi}{2}-\beta\right)\right] + \frac{G_D}{2} = G_D\left[\frac{1+\cos(\beta)}{2}\right] \tag{2.93}$$

Similarly, the ground-reflected radiation is obtained by $\rho_G(G_B + G_D)$, where ρ_G is ground albedo. Therefore, G_{Gt} is obtained as follows.

Ground-reflected radiation,

$$\rho_G(G_B + G_D) = 2\int_0^{\pi/2} G_r\cos(\Phi)\, d\Phi = 2G_r \tag{2.94}$$

where G_r is the isotropic ground-reflected radiance (W/m^2 rad).

Ground-reflected radiation on tilted surfaces,

$$G_{Gt} = \int_{\pi/2-\beta}^{\pi/2} G_r\cos(\Phi)\, d\Phi \tag{2.95}$$

Combining Eqns (2.94) and (2.95) as before,

$$G_{Gt} = \rho_G(G_B + G_D)\left[\frac{1-\cos(\beta)}{2}\right] \tag{2.96}$$

Therefore, inserting Eqns (2.93) and (2.96) into Eq. (2.85), we get:

$$G_t = R_B G_B + G_D\left[\frac{1+\cos(\beta)}{2}\right] + (G_B + G_D)\rho_G\left[\frac{1-\cos(\beta)}{2}\right] \tag{2.97}$$

The total radiation on a horizontal surface, G, is the sum of horizontal beam and diffuse radiation; that is,

$$G = G_B + G_D \tag{2.98}$$

Therefore, Eq. (2.97) can also be written as:

$$R = \frac{G_t}{G} = \frac{G_B}{G}R_B + \frac{G_D}{G}\left[\frac{1+\cos(\beta)}{2}\right] + \rho_G\left[\frac{1-\cos(\beta)}{2}\right] \tag{2.99}$$

where R is called the *total radiation tilt factor.*

Other radiation models

The isotropic sky model is the simplest model that assumes that all diffuse radiation is uniformly distributed over the sky dome and that reflection on the ground is diffuse. A number of other models have been developed by a number of researchers. Three of these models are summarized in this section: the Klucher model, the Hay–Davies model, and the Reindl model. The latter proved to give very good results in the Mediterranean region.

Klucher model

Klucher (1979) found that the isotopic model gives good results for overcast skies but underestimates irradiance under clear and partly overcast conditions, when there is increased intensity near the horizon and in the circumsolar region of the sky. The model developed by Klucher gives the total irradiation on a tilted plane:

$$G_t = G_B R_B + G_D \left[\frac{1+\cos(\beta)}{2}\right]\left[1 + F' \sin^3\left(\frac{\beta}{2}\right)\right]\left[1 + F' \cos^2(\beta)\sin^3(\Phi)\right] + (G_B + G_D)\rho\left[\frac{1-\cos(\beta)}{2}\right] \tag{2.100}$$

where F' is a clearness index given by:

$$F' = 1 - \left(\frac{G_D}{G_B + G_D}\right)^2 \tag{2.101}$$

The first of the modifying factors in the sky diffuse component takes into account horizon brightening; the second takes into account the effect of circumsolar radiation. Under overcast skies, the clearness index F' becomes 0 and the model reduces to the isotropic model.

Hay–Davies model

In the Hay–Davies model, diffuse radiation from the sky is composed of an isotropic and circumsolar component (Hay and Davies, 1980) and horizon brightening is not taken into account. The anisotropy index, A, defined in Eq. (2.102), represents the transmittance through atmosphere for beam radiation:

$$A = \frac{G_{Bn}}{G_{on}} \tag{2.102}$$

The anisotropy index is used to quantify the portion of the diffuse radiation treated as circumsolar, with the remaining portion of diffuse radiation assumed isotropic. The circumsolar component is assumed to be from the sun's position. The total irradiance is then computed by:

$$G_t = (G_B + G_D A)R_B + G_D(1-A)\left[\frac{1+\cos(\beta)}{2}\right] + (G_B + G_D)\rho\left[\frac{1-\cos(\beta)}{2}\right] \tag{2.103}$$

Reflection from the ground is dealt with as in the isotropic model.

Reindl model

In addition to isotropic diffuse and circumsolar radiation, the Reindl model also accounts for horizon brightening (Reindl et al., 1990a,b) and employs the same definition of the anisotropy index, A, as described in Eq. (2.102). The total irradiance on a tilted surface can then be calculated using:

$$G_t = (G_B + G_D A)R_B + G_D(1-A)\left[\frac{1-\cos(\beta)}{2}\right]\left[1 + \sqrt{\frac{G_B}{G_B + G_D}}\sin^3\left(\frac{\beta}{2}\right)\right] + (G_B + G_D)\rho\left[\frac{1-\cos(\beta)}{2}\right] \tag{2.104}$$

Reflection on the ground is again dealt with as in the isotropic model. Due to the additional term in Eq. (2.104), representing horizon brightening, the Reindl model provides slightly higher diffuse irradiances than the Hay–Davies model.

Insolation on tilted surfaces

The amount of insolation on a terrestrial surface at a given location and time depends on the orientation and slope of the surface. In the case of flat-plate collectors installed at a certain fixed angle, system designers need to have data about the solar radiation on the surface of the collector. Most measured data, however, are for either normal incidence or horizontal. Therefore, it is often necessary to convert these data to radiation on tilted surfaces. Based on these data, a reasonable estimation of radiation on tilted surfaces can be made. An empirical method for the estimation of the monthly average daily total radiation incident on a tilted surface was developed by Liu and Jordan (1977). In their correlation, the diffuse to total radiation ratio for a horizontal surface is expressed in terms of the monthly clearness index, $\overline{K}_{\mathrm{T}}$, with the following equation:

$$\frac{\overline{H}_{\mathrm{D}}}{\overline{H}} = 1.390 - 4.027\overline{K}_{\mathrm{T}} + 5.531\overline{K}_{\mathrm{T}}^2 - 3.108\overline{K}_{\mathrm{T}}^3 \tag{2.105a}$$

Collares-Pereira and Rabl (1979) expressed the same parameter by also considering the sunset hour angle:

$$\frac{\overline{H}_{\mathrm{D}}}{\overline{H}} = 0.775 + 0.00653(h_{\mathrm{ss}} - 90) - [0.505 + 0.00455(h_{\mathrm{ss}} - 90)]\cos\left(115\overline{K}_T - 103\right) \tag{2.105b}$$

where

h_{ss} = sunset hour angle (degrees).

Erbs et al. (1982) also expressed the monthly average daily diffuse correlations by taking into account the season, as follows

For $h_{\mathrm{ss}} \leq 81.4^\circ$ and $0.3 \leq \overline{K}_{\mathrm{T}} \leq 0.8$,

$$\frac{\overline{H}_{\mathrm{D}}}{\overline{H}} = 1.391 - 3.560\overline{K}_{\mathrm{T}} + 4.189\overline{K}_{\mathrm{T}}^2 - 2.137\overline{K}_{\mathrm{T}}^3 \tag{2.105c}$$

For $h_{\mathrm{ss}} > 81.4^\circ$ and $0.3 \leq \overline{K}_{\mathrm{T}} \leq 0.8$,

$$\frac{\overline{H}_{\mathrm{D}}}{\overline{H}} = 1.311 - 3.022\overline{K}_{\mathrm{T}} + 3.427\overline{K}_{\mathrm{T}}^2 - 1.821\overline{K}_{\mathrm{T}}^3 \tag{2.105d}$$

With the monthly average daily total radiation $\overline{H}$ and the monthly average daily diffuse radiation $\overline{H}_{\mathrm{D}}$ known, the monthly average beam radiation on a horizontal surface can be calculated by:

$$\overline{H}_{\mathrm{B}} = \overline{H} - \overline{H}_{\mathrm{D}} \tag{2.106}$$

Like Eq. (2.99), the following equation may be written for the monthly total radiation tilt factor $\overline{R}$:

$$\overline{R} = \frac{\overline{H}_{\mathrm{t}}}{\overline{H}} = \left(1 - \frac{\overline{H}_{\mathrm{D}}}{\overline{H}}\right)\overline{R}_{\mathrm{B}} + \frac{\overline{H}_{\mathrm{D}}}{\overline{H}}\left[\frac{1 + \cos(\beta)}{2}\right] + \rho_{\mathrm{G}}\left[\frac{1 - \cos(\beta)}{2}\right] \tag{2.107}$$

where

$\overline{H}_{\mathrm{t}}$ = monthly average daily total radiation on a tilted surface (MJ/m^2 day).

$\overline{R}_{\mathrm{B}}$ = monthly mean beam radiation tilt factor.

The term $\overline{R}_B$ is the ratio of the monthly average beam radiation on a tilted surface to that on a horizontal surface. Actually, this is a complicated function of the atmospheric transmittance, but according to Liu and Jordan (1977), it can be estimated by the ratio of extraterrestrial radiation on the tilted surface to that on a horizontal surface for the month. For surfaces facing directly toward the equator, it is given by:

$$\overline{R}_B = \frac{\cos(L-\beta)\cos(\delta)\sin(h'_{ss}) + (\pi/180)h'_{ss}\sin(L-\beta)\sin(\delta)}{\cos(L)\cos(\delta)\sin(h_{ss}) + (\pi/180)h_{ss}\sin(L)\sin(\delta)} \tag{2.108}$$

where h'_{ss} is sunset hour angle on the tilted surface (degrees), given by:

$$h'_{ss} = \min\{h_{ss}, \cos^{-1}[-\tan(L-\beta)\tan(\delta)]\} \tag{2.109}$$

It should be noted that, for the Southern Hemisphere, the term $(L-\beta)$ of Eqs (2.108) and (2.109) changes to $(L+\beta)$.

For the same days as those shown in Table 2.5, the monthly average terrestrial insolation on a tilted surface for various months for latitudes $-60°$ to $+60°$ and for a slope equal to latitude and latitude plus 10°, which is the usual collector inclination for solar water-heating collectors, is shown in Appendix 3, Figures A3.6 and A3.7, respectively.

EXAMPLE 2.20

For July, estimate the monthly average daily total solar radiation on a surface facing south, tilted 45°, and located at 35°N latitude. The monthly average daily insolation on a horizontal surface is 23.14 MJ/m^2 day. Ground reflectance is equal to 0.2.

Solution

From Example 2.18, we have: $\overline{H}_D/\overline{H} = 0.316$, $\delta = 21.2°$, and $h_{ss} = 106°$. The sunset hour angle for a tilted surface is given by Eq. (2.109):

$$h'_{ss} = \min\{h_{ss}, \cos^{-1}[-\tan(L-\beta)\tan(\delta)]\}$$

Here, $\cos^{-1}[-\tan(35-45)\tan(21.2)] = 86°$. Therefore,

$$h'_{ss} = 86°$$

The factor $\overline{R}_B$ is calculated from Eq. (2.108) as:

$$\overline{R}_B = \frac{\cos(L-\beta)\cos(\delta)\sin(h'_{ss}) + (\pi/180)h'_{ss}\sin(L-\beta)\sin(\delta)}{\cos(L)\cos(\delta)\sin(h_{ss}) + (\pi/180)h_{ss}\sin(L)\sin(\delta)}$$

$$= \frac{\cos(35-45)\cos(21.2)\sin(86) + (\pi/180)(86)\sin(35-45)\sin(21.2)}{\cos(35)\cos(21.2)\sin(106) + (\pi/180)(106)\sin(35)\sin(21.2)} = 0.735$$

From Eq. (2.107),

$$\overline{R} = \left(1 - \frac{\overline{H}_D}{\overline{H}}\right)\overline{R}_B + \frac{\overline{H}_D}{\overline{H}}\left[\frac{1+\cos(\beta)}{2}\right] + \rho_G\left[\frac{1-\cos(\beta)}{2}\right]$$

$$= (1-0.316)(0.735) + 0.316\left[\frac{1+\cos(45)}{2}\right] + 0.2\left[\frac{1-\cos(45)}{2}\right] = 0.802$$

Finally, the average daily total radiation on the tilted surface for July is:

$$\overline{H}_t = \overline{RH} = 0.802(23.14) = 18.6\ \text{MJ/m}^2\ \text{day}$$

2.3.9 Solar radiation measuring equipment

A number of radiation parameters are needed for the design, sizing, performance evaluation, and research of solar energy applications. These include total solar radiation, beam radiation, diffuse radiation, and sunshine duration. Various types of equipment measure the instantaneous and long-term integrated values of beam, diffuse, and total radiation incident on a surface. This equipment usually employs the thermoelectric and photovoltaic effects to measure the radiation. Detailed description of this equipment is not within the scope of this book; this section is added, however, so the reader might know the types of available equipment. More details of this equipment can easily be found from manufacturers' catalogues on the Internet.

There are basically two types of solar radiation measuring instruments: the pyranometer (see Figure 2.29) and the pyrheliometer (see Figure 2.30). The former is used to measure total (beam and diffuse) radiation within its hemispherical field of view, whereas the latter is an instrument used for measuring the direct solar irradiance. The pyranometer can also measure the diffuse solar radiation if the sensing element is shaded from the beam radiation (see Figure 2.31). For this purpose a shadow band is mounted with its axis tilted at an angle equal to the latitude of the location plus the declination for the day of measurement. Since the shadow band hides a considerable portion of the sky, the measurements require corrections for that part of diffuse radiation obstructed by the band. Pyrheliometers are used to measure direct solar irradiance, required primarily to predict the performance of concentrating solar collectors. Diffuse radiation is blocked by mounting the sensor element at the bottom of a tube pointing directly at the sun. Therefore, a two-axis sun-tracking system is required to measure the beam radiation.

Finally, sunshine duration is required to estimate the total solar irradiation. The duration of sunshine is defined as the time during which the sunshine is intense enough to cast a shadow. Also, the duration of sunshine has been defined by the World Meteorological Organization as the time during which the beam solar irradiance exceeds the level of 120 W/m^2. Two types of sunshine recorders are used: the focusing type and a type based on the photoelectric effect. The focusing type consists of a solid glass sphere, approximately 10 cm in diameter, mounted concentrically in a section of a spherical bowl whose diameter is such that the sun's rays can be focused on a special card with time marking, held in place by grooves in the bowl. The record card is burned whenever bright sunshine exists. Thus, the portion of the burned trace provides the duration of sunshine for the day. The sunshine recorder based on the photoelectric effect consists of two photovoltaic cells, with one cell exposed to the beam

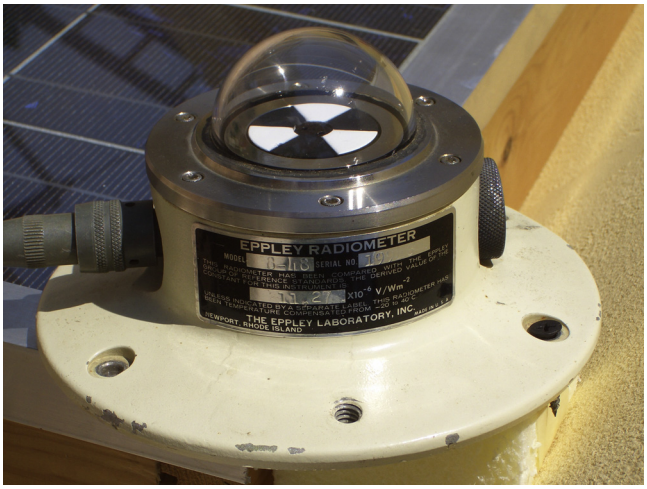

FIGURE 2.29

Photograph of a pyranometer.

FIGURE 2.30

Photograph of a solar pyrheliometer.

solar radiation and the other cell shaded from it by a shading ring. The radiation difference between the two cells is a measure of the duration of sunshine.

The International Standards Organization (ISO) published a series of international standards specifying methods and instruments for the measurement of solar radiation. These are

- **ISO 9059** (1990). *Calibration of field pyrheliometers by comparison to a reference pyrheliometer.* This International Standard describes the calibration of field pyrheliometers using reference pyrheliometers and sets out the calibration procedures and the calibration hierarchy for the transfer of the calibration. This International Standard is mainly intended for use by calibration services and test laboratories to enable a uniform quality of accurate calibration factors to be achieved.
- **ISO 9060** (1990). *Specification and classification of instruments for measuring hemispherical solar and direct solar radiation*. This standard establishes a classification and specification of instruments for the measurement of hemispherical solar and direct solar radiation integrated

FIGURE 2.31

Photograph of a pyranometer with shading ring for measuring diffuse solar radiation.

over the spectral range from 0.3 to 3 μm. According to the standard, pyranometers are radiometers designed for measuring the irradiance on a plane receiver surface, which results from the radiant fluxes incident from the hemisphere above, within the required wavelength range. Pyrheliometers are radiometers designed for measuring the irradiance that results from the solar radiant flux from a well-defined solid angle, the axis of which is perpendicular to the plane receiver surface.

- **ISO 9846** (1993). *Calibration of a pyranometer using a pyrheliometer.* This standard also includes specifications for the shade ring used to block the beam radiation, the measurement of diffuse radiation, and support mechanisms of the ring.
- **IS0 9847** (1992). *Calibration of field pyranometers by comparison to a reference pyranometer.* According to the standard, accurate and precise measurements of the irradiance of the global (hemispheric) solar radiation are required in:

  1. The determination of the energy available to flat-plate solar collectors.
  2. The assessment of irradiance and radiant exposure in the testing of solar- and non-solar-related material technologies.
  3. The assessment of the direct versus diffuse solar components for energy budget analysis, for geographic mapping of solar energy, and as an aid in the determination of the concentration of aerosol and particulate pollution and the effects of water vapor.

Although meteorological and resource assessment measurements generally require pyranometers oriented with their axes vertical, applications associated with flat-plate collectors and the study of the solar exposure of related materials require calibrations of instruments tilted at a predetermined non-vertical orientation. Calibrations at fixed tilt angles have applications that seek state-of-the-art accuracy, requiring corrections for cosine, tilt, and azimuth.

Finally, the International Standards Organization published a technical report, "lSO/TR 9901: *1990—Field pyranometers—Recommended practice for use*," the scope of which is self-explanatory.

2.4 The solar resource

The operation of solar collectors and systems depends on the solar radiation input and the ambient air temperature and their sequences. One of the forms in which solar radiation data are available is on maps. These give the general impression of the availability of solar radiation without details on the local meteorological conditions and, for this reason, must be used with care. One valuable source of such information is the Meteonorm. Two maps showing the annual mean global solar radiation for the years 1981–2000 for Europe and North America are shown in Figures 2.32 and 2.33, respectively (Meteonorm, 2009). These are based on numerous climatological databases and computational models. Maps for other regions of the world can be obtained from the Meteonorm web site (Meteonorm, 2009).

Another way of estimating the average solar radiation $\overline{H}$ is by the use of the following equation (Page, 1964):

$$\overline{K}_{\mathrm{T}} = \frac{\overline{H}}{\overline{H}_{\mathrm{o}}} = a + b\frac{\overline{n}}{\overline{N}} \tag{2.110}$$

where

a and b = empirical constants
$\overline{n}$ = monthly average daily hours of sunshine
$\overline{N}$ = monthly average maximum possible daily hours of sunshine, given by the day length (Eq. (2.17)) of the average day of each month shown in Table 2.1.

As was seen before values of $\overline{H}_{\mathrm{o}}$ can be obtained from Eq. (2.79) and for the average day of each month values can be obtained directly from Table 2.5. The constants a and b can be obtained from published tables or can be estimated from measured data in a location.

For the local climate, data in the form of a TMY are usually required. This is a typical year, which is defined as a year that sums up all the climatic information characterizing a period as long as the mean life of a solar system. In this way, the long-term performance of a collector or a system can be calculated by running a computer program over the reference year.

2.4.1 Typical meteorological year

A representative database of weather data for 1-year duration is known as the *test reference year* (TRY) or *typical meteorological year* (TMY). A TMY is a data set of hourly values of solar radiation and meteorological elements. It consists of months selected from individual years concatenated to form a

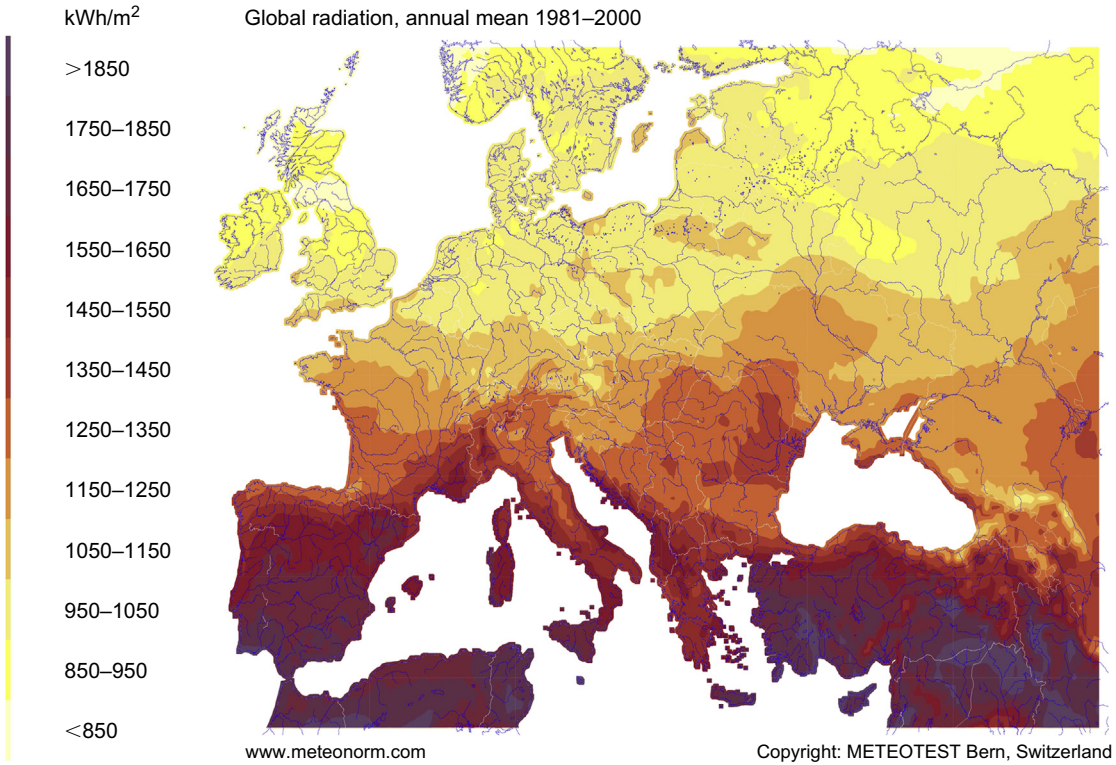

FIGURE 2.32

Annual total solar irradiation on horizontal surface for Europe.

Source: Meteonorm database of Meteotest (www.Meteonorm.com).

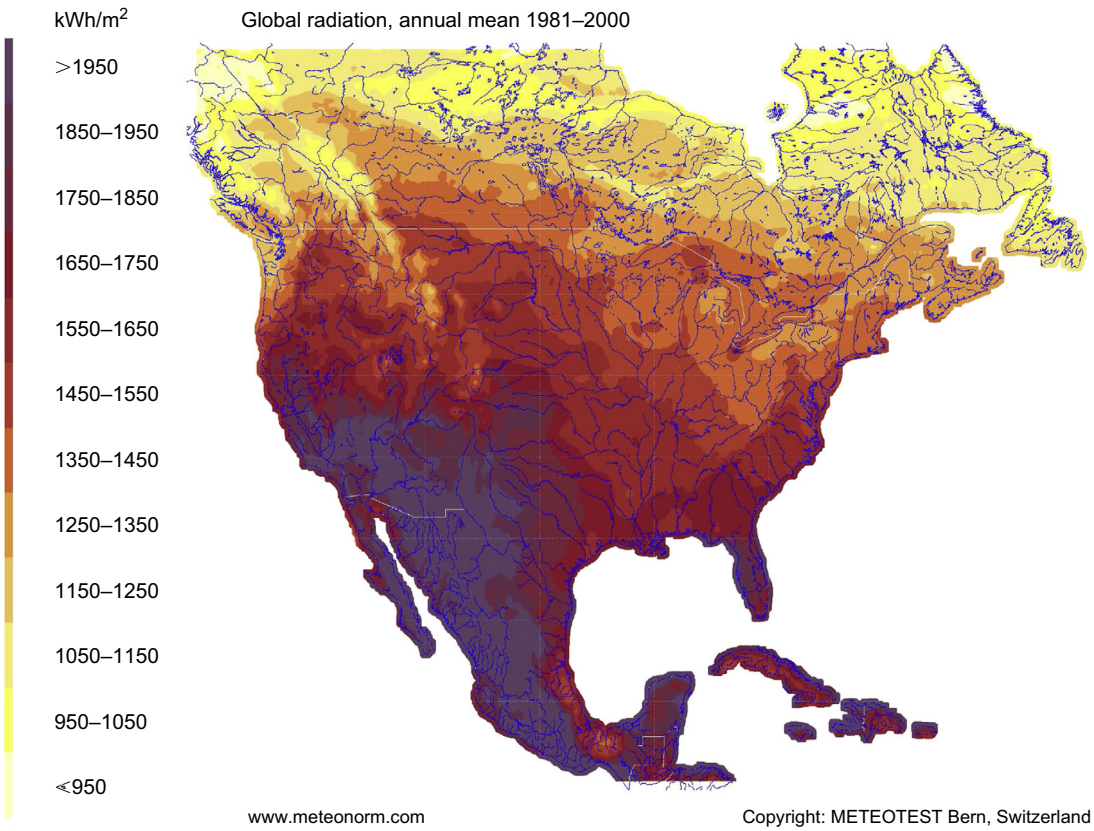

FIGURE 2.33

Annual total solar irradiation on horizontal surface for North America.

Source: Meteonorm database of Meteotest (www.Meteonorm.com).

complete year. The TMY contains values of solar radiation (global on horizontal and direct), ambient temperature, relative humidity, and wind speed and direction for all hours of the year. The selection of typical weather conditions for a given location is very crucial in computer simulations to predict the performance of solar systems and the thermal performance of buildings and has led various investigators to either run long periods of observational data or select a particular year that appears to be typical from several years of data. The intended use of a TMY file is for computer simulations of solar energy conversion systems and building systems (see Chapter 11, Section 11.5).

The adequacy of using an average or typical year of meteorological data with a simulation model to provide an estimate of the long-term system performance depends on the sensitivity of system performance to the hourly and daily weather sequences. Regardless of how it is selected, an "average" year cannot be expected to have the same weather sequences as those occurring over the long term. However, the simulated performance of a system for an "average year" may provide a good estimate of the long-term system performance, if the weather sequences occurring in the average year are

representative of those occurring over the long term or the system performance is independent of the weather sequences (Klein et al., 1976). Using this approach, the long-term integrated system performance can be evaluated and the dynamic system's behavior can be obtained.

In the past, many attempts were made to generate such climatological databases for different areas around the world using various methodologies. One of the most common methodologies for generating a TMY is the one proposed by Hall et al. (1978) using the Filkenstein–Schafer (FS) statistical method (Filkenstein and Schafer, 1971).

The FS method algorithm is as follows: First, the cumulative distribution functions (CDFs) are calculated for each selected meteorological parameter and for each month, over the whole selected period as well as over each specific year of the period. To calculate the CDFs for each parameter, the data are grouped in a number of bins, and the CDFs are calculated by counting the cases in the same bin.

The next step is to compare the CDF of a meteorological parameter, such as global horizontal radiation, for each month for each specific year with the respective CDF of the long-term composite of all years in the selected period.

The FS is the mean difference of the long-term CDF, CDF_{LT}, and the specific month's CDF, CDF_{SM}, calculated in the bins used for the estimation of the CDFs, given by:

$$FS = \frac{1}{N}\sum_{i=1}^{N}|CDF_{LT}(z_i) - CDF_{SM}(z_i)| \tag{2.111}$$

where

N = number of bins (by default, $N = 31$).
z_i = value of the FS statistic for the particular month of the specific year and the meteorological parameter under consideration.

The next step is the application of the weighting factors, WF_j, to the FS statistics values, one for each of the considered meteorological parameters, FS_j, corresponding to each specific month in the selected period. In this way, a weighted sum, or average value, WS, is derived and this value is assigned to the respective month; that is,

$$WS = \frac{1}{M}\sum_{j=1}^{M} WF_j FS_j \tag{2.112}$$

with

$$\sum_{j=1}^{M} WF_i = 1 \tag{2.113}$$

where

M = number of parameters in the database.

The user can change the WF values, thus examining the relative importance of each meteorological parameter in the final result. The smaller the WS, the better the approximation to a typical meteorological month (TMM).

Applying this procedure for all months of the available period, a composite year can be formed consisting of the selected months with the smallest WS values.

Table 2.6 Format of TMY File Suitable for the TRNSYS Program Up to Version 14

Month of Year	Hour of Month	I_B (kJ/m^2)[a]	I (kJ/m^2)[b]	Dry Bulb Temp[c]	H_R[d]	Wind Velocity (m/s)	Wind Direction[e]
1	1	0	0	75	60.47	1	12
1	2	0	0	75	60.47	1	12
1	3	0	0	70	57.82	1	12
1	4	0	0	70	57.82	1	12
1	5	0	0	75	58.56	2	12
—	—	—	—	—	—	—	—
12	740	0	0	45	47.58	1	23
12	741	0	0	30	43.74	1	25
12	742	0	0	20	40.30	1	26
12	743	0	0	20	40.30	1	27
12	744	0	0	10	37.51	1	23

[a] I_B = *Direct (beam) normal solar radiation (integrated over previous hour) in kJ/m^2.*
[b] I = *Global solar radiation on horizontal (integrated over previous hour) in kJ/m^2.*
[c] *Degrees ×10 (°C).*
[d] *Humidity ratio (H_R) in kg of water/kg of air ×°10,000.*
[e] *Degrees ÷ 10, expressed as 0 for wind from north, 9 for east, 18 for south, and so forth.*

The root mean standard deviation (RMSD) of the total daily values of the global solar irradiance distribution for each month of each year can then be estimated with respect to the mean long-term hourly distribution and the FS statistics. The RMSD can be computed, and for each month, the year corresponding to the lowest value can be selected. The estimations are carried out according to the expression:

$$\mathrm{RMSD} = \sqrt{\frac{\sum_{i=1}^{N}(x_i - \overline{x})}{N}} \tag{2.114}$$

where $\overline{x}$ = the average value of its parameter over the number of bins ($N = 31$).

A total of 8760 rows are included in a TMY file, each corresponding to an hour of the year. The format of TMY file suitable for earlier versions of the TRNSYS program is shown in Table 2.6.

2.4.2 Typical meteorological year, second generation

A type 2 TMY format is completely different and consists of many more fields. Such a file can be used with detailed building analysis programs such as TRNSYS (version 16), DOE-2, BDA (Building Design Advisor), and Energy Plus. A TMY-2 file also contains a complete year (8760 items of data) of hourly meteorological data. Each hourly record in the file contains values for solar radiation, dry bulb temperature, and meteorological elements, such as illuminance, precipitation, visibility, and snowfall. Radiation and illumination data are becoming increasingly necessary in many simulation programs. A two-character source and an uncertainty flag are attached to each data value to indicate whether the

Table 2.7 Header Elements in the TMY-2 Format (First Record Only)

Field Position	Element	Definition	Value Used
002–006	5-Digit number	Weather station's number	17609
008–029	City	City where the station is located (maximum 22 characters)	Nicosia
031–032	State	State where the station is located (2-letter abbreviation)	—
034–036	Time zone	Time zone: number of hours by which the local standard time is ahead of Greenwich (+ve E, −ve W)	2
038–044	Latitude	Latitude of the station:	
038		N = north of equator	N
040–041		Degrees	34
043–044		Minutes	53
046–053	Longitude	Longitude of the station:	
046		W = west, E = east	E
048–050		Degrees	33
052–053		Minutes	38
056–059	Elevation	Elevation of station in meters above sea level	162

data value was measured, modeled, or missing and provide an estimate of the uncertainty of the data value. By including the uncertainty flags, users can evaluate the potential impact of weather variability on the performance of solar systems or buildings.

The first record of each file is the file header that describes the station. The file header contains a five-digit meteorological station number, city, state (optional), time zone, latitude, longitude, and elevation. The field positions and definitions of these header elements, together with the values given for the TMY2 for Nicosia, Cyprus (Kalogirou, 2003), are shown in Table 2.7.

Following the file header, 8760 hourly data records provide a 1-year record of solar radiation, illuminance, and meteorological data, along with their source and uncertainty flags. Table 2.8 gives field positions and element definitions of each hourly record (Marion and Urban, 1995). Each hourly record begins with the year (field positions 2–3) from which the typical month was chosen, followed by the month, day, and hour information and the rest of the data as shown in Table 2.8 (Kalogirou, 2003).

For solar radiation and illuminance elements, the data values represent the energy received during the 60 min preceding the hour indicated. For meteorological elements (with a few exceptions), observations or measurements were made at the hour indicated. A few of the meteorological elements have observations, measurements, or estimates made at daily, instead of hourly, intervals. Consequently, the data values for broadband aerosol optical depth, snow depth, and days since last snowfall represent the values available for the day indicated.

With the exception of extraterrestrial horizontal and extraterrestrial direct radiation, the two field positions immediately following the data value provide source and uncertainty flags both to indicate whether the data were measured, modeled, or missing and to provide an estimate of the uncertainty of

Table 2.8 Data Elements in the TMY-2 Format (All Except the First Record)

Field Position	Element	Value	Definition
002–009	Local standard time		
002–003	Year	2-Digit	Year
004–005	Month	1–12	Month
006–007	Day	1–31	Day of month
008–009	Hour	1–24	Hour of day in local standard time
010–013	Extraterrestrial horizontal irradiation	0–1415	Amount of solar radiation in Wh/m^2 received on a horizontal surface at the top of the atmosphere
014–017	Extraterrestrial direct normal irradiation	0–1415	Amount of solar radiation in Wh/m^2 received on a surface normal to the sun at the top of the atmosphere
018–023	Global horizontal irradiation		Total amount of direct and diffuse solar radiation in Wh/m^2 received on a horizontal surface
018–021	Data value	0–1200	
022	Flag for data source	A–H, ?	
023	Flag for data uncertainty	0–9	
024–029	Direct normal irradiation		Amount of solar radiation in Wh/m^2 received within a 5.7° field of view centered on the sun
024–027	Data value	0–1100	
028	Flag for data source	A–H, ?	
029	Flag for data uncertainty	0–9	
030–035	Diffuse horizontal irradiation		Amount of solar radiation in Wh/m^2 received from the sky (excluding the solar disk) on a horizontal surface
030–033	Data value	0–700	
034	Flag for data source	A–H, ?	
035	Flag for data uncertainty	0–9	
036–041	Global horizontal illuminance		Average total amount of direct and diffuse illuminance in hundreds of lux received on a horizontal surface
036–039	Data value	0–1300	0 to 1300 = 0 to 130,000 lux
040	Flag for data source	I, ?	
041	Flag for data uncertainty	0–9	

Continued

Table 2.8 Data Elements in the TMY-2 Format (All Except the First Record)—*Continued*

Field Position	Element	Value	Definition
042–047	Direct normal illuminance		Average amount of direct normal illuminance in hundreds of lux received within a 5.7° field of view centered on the sun
042–045	Data value	0–1100	0 to 1100 = 0 to 110,000 lux
046	Flag for data source	I, ?	
047	Flag for data uncertainty	0–9	
048–053	Diffuse horizontal illuminance		Average amount of illuminance in hundreds of lux received from the sky (excluding the solar disk) on a horizontal surface
048–051	Data value	0–800	0 to 800 = 0 to 80,000 lux
052	Flag for data source	I, ?	
053	Flag for data uncertainty	0–9	
054–059	Zenith luminance		Average amount of luminance at the sky's zenith in tens of Cd/m^2
054–057	Data value	0–7000	0 to 7000 = 0 to 70,000 Cd/m^2
058	Flag for data source	I, ?	
059	Flag for data uncertainty	0–9	
060–063	Total sky cover		Amount of sky dome in tenths covered by clouds or obscuring phenomena at the hour indicated
060–061	Data value	0–10	
062	Flag for data source	A–F	
063	Flag for data uncertainty	0–9	
064–067	Opaque sky cover		Amount of sky dome in tenths covered by clouds or obscuring phenomena that prevent observing the sky or higher cloud layers at the hour indicated
064–065	Data value	0–10	
066	Flag for data source	A–F	
067	Flag for data uncertainty	0–9	
068–073	Dry bulb temperature		Dry bulb temperature in tenths of a degree Centigrade at the hour indicated.

Table 2.8 Data Elements in the TMY-2 Format (All Except the First Record)—*Continued*

Field Position	Element	Value	Definition
068–071	Data value	−500 to 500	−500 to 500 = −50.0 to 50.0 °C
072	Flag for data source	A–F	
073	Flag for data uncertainty	0–9	
074–079	Dew point temperature		Dew point temperature in tenths of a degree Centigrade at the hour indicated.
074–077	Data value	−600 to 300	−600 to 300 = −60.0 to 30.0 °C
078	Flag for data source	A–F	
079	Flag for data uncertainty	0–9	
080–084	Relative humidity		Relative humidity in percent at the hour indicated
080–082	Data value	0–100	
083	Flag for data source	A–F	
084	Flag for data uncertainty	0–9	
085–090	Atmospheric pressure		Atmospheric pressure at station in mbar at the hour indicated
085–088	Data value	700–1100	
089	Flag for data source	A–F	
090	Flag for data uncertainty	0–9	
091–095	Wind direction		Wind direction in degrees at the hour indicated. (N = 0 or 360, E = 90, S = 180, W = 270). For calm winds, wind direction equals zero.
091–093	Data value	0–360	
094	Flag for data source	A–F	
095	Flag for data uncertainty	0–9	
096–100	Wind speed		Wind speed in tenths of meters per second at the hour indicated.
096–98	Data value	0–400	0 to 400 = 0 to 40.0 m/s
99	Flag for data source	A–F	
100	Flag for data uncertainty	0–9	
101–106	Visibility		Horizontal visibility in tenths of kilometers at the hour indicated.
101–104	Data value	0–1609	7777 = unlimited visibility
105	Flag for data source	A–F, ?	0 to 1609 = 0.0 to 160.9 km
106	Flag for data uncertainty	0–9	9999 = missing data

Continued

Table 2.8 Data Elements in the TMY-2 Format (All Except the First Record)—*Continued*

Field Position	Element	Value	Definition
107–113	Ceiling height		Ceiling height in meters at the hour indicated.
107–111	Data value	0–30,450	77777 = unlimited ceiling height
112	Flag for data source	A–F, ?	88888 = cirroform
113	Flag for data uncertainty	0–9	99999 = missing data
114–123	Present weather	–	Present weather conditions denoted by a 10-digit number.
124–128	Precipitable water		Precipitation water in millimeters at the hour indicated
124–126	Data value	0–100	
127	Flag for data source	A–F	
128	Flag for data uncertainty	0–9	
129–133	Aerosol optical depth		Broadband aerosol optical depth (broadband turbidity) in thousandths on the day indicated.
129–131	Data value	0–240	0 to 240 = 0.0 to 0.240
132	Flag for data source	A–F	
133	Flag for data uncertainty	0–9	
134–138	Snow depth		Snow depth in centimeters on the day indicated.
134–136	Data value	0–150	999 = missing data
137	Flag for data source	A–F, ?	
138	Flag for data uncertainty	0–9	
139–142	Days since last snowfall		Number of days since last snowfall.
139–140	Data value	0–88	88 = 88 or greater days
141	Flag for data source	A–F, ?	99 = missing data
142	Flag for data uncertainty	0–9	

From Marion and Urban (1995).

the data. Source and uncertainty flags for extraterrestrial horizontal and extraterrestrial direct radiation are not provided, because these elements were calculated using equations considered to give exact values. Explanation of the uncertainty flags for the other quantities is given in Marion and Urban (1995).

A sample of the Nicosia TMY-2 file, showing the data for the first days of January, including the header elements, can be seen in Figure 2.34 (Kalogirou, 2003). It should be noted that the format of the

```
 17609 NICOSIA                    2 N 34 53 E 33 38   162
 86 1 1 1   01415   0?9   0?9   0?9   0?9   0?9   0?9   0?9 5B8 2B8  75C9  65C9 94C91021C9120*0 10B8 233B877777*09999999999  0*0 70E8  0*088*0
 86 1 1 2   01415   0?9   0?9   0?9   0?9   0?9   0?9   0?9 4B8 2B8  75C9  65C9 94C91021C9120*0 10B8 217B877777*09999999999  0*0 70E8  0*088*0
 86 1 1 3   01415   0?9   0?9   0?9   0?9   0?9   0?9   0?9 4A7 1A7  70C9  62C9 93C91021C9120A7 10A7 200A722000A79999999999  0*0 70E8  0*088*0
 86 1 1 4   01415   0?9   0?9   0?9   0?9   0?9   0?9   0?9 4B8 1B8  70C9  59C9 93C91021C9120*0 20B8 333B822000*09999999999  0*0 70E8  0*088*0
 86 1 1 5   01415   0?9   0?9   0?9   0?9   0?9   0?9   0?9 3B8 1B8  75C9  60C9 92C91021C9120*0 10B8 467B822000*09999999999  0*0 70E8  0*088*0
 86 1 1 6   01415   1?9   0?9   0?9   0?9   0?9   0?9   0?9 3B8 1A7  75C9  61C9 91C91021C9120A7 10A7 600A722000A79999999999  0*0 70E8  0*088*0
 86 1 1 7   01415 19H9   0H9   0H9   0I9   0I9   0I9   0I9 3B8 2B8  90B8  65C8 89E81021B8120*0 10B8 600B822000*09999999999  0*0 70E8  0*088*0
 86 1 1 8 1401415  70H9   0H9  70H9  52I9  53I9  47I9  68I9 3B8 2B8  90B8  69C8 87E81021B8120*0 10B8 600B822000*09999999999  0*0 70E8  0*088*0
 86 1 1 9 3731415  89G9   0G9  89G9 221I9 369I9 118I9 161I9 2A7 2A7 120A7  77A7 83E81022E8120A7 20A7 600A722000A79999999999  0*0 70E8  0*088*0
 86 1 110 5601415  78H9   0H9  78H9 382I9 647I9 126I9 168I9 3B8 2B8 120B8  84C8 79E81021B8 80*0 20B8 533B822000*09999999999  0*0 70E8  0*088*0
```

FIGURE 2.34

Format of TMY-2 file.

TMY-2 for the Energy Plus program is a little different than the one shown in Figure 2.34 since it includes after the header design conditions, extreme periods and holidays, and daylight saving data.

2.4.3 Typical meteorological year, third generation

The changes between TMY-2 and TMY-3 concern the format of the file and minor changes to the algorithm in selecting typical months. The latter concern changes to the persistence criteria implemented, which better accommodates the selection a TMM for periods or records with fewer years. Additionally, the code which prioritized the selection of months with measured solar data was removed. The effects of these changes between the TMY-2 and TMY-3 algorithm were evaluated as part of the TMY-3 production process (Wilcox and Marion, 2008). In particular, a few changes from the TMY-2 procedures were required to accommodate the use of data derived from only a 15-year period. For TMY-2 data, months with measured solar radiation data were preferred for selection as a typical month. TMY-3 procedures do not include this criterion because only modeled solar radiation data are included in the TMY-3 data to provide more consistent solar radiation values. For the TMY-3 data, using only 15 years instead of 30 years to select a candidate month, require that the persistence checks are relaxed to ensure that a candidate month could be selected. For the TMY-2 data, a candidate month is excluded from further consideration if it is the month with the most runs. For TMY-3, a candidate month is only excluded if it has more runs than every other candidate month. Consequently, if two candidate months tie for the most runs, neither is removed by the TMY-3 procedure, whereas the TMY-2 procedure would get rid of both candidate months. As an additional step, if the TMY-3 persistence procedure eliminates all candidate months, persistence was ignored and a month was selected from the candidate months that was closest to the long-term mean and median. This ensured the selection of a typical month for TMY-3 using 15-year or shorter data sets. No TMY for a site was produced however, if the pool of data was less than 10 years (Wilcox and Marion, 2008).

Generally, except for a few changes to the weighting criteria, which account for the relative importance of the solar radiation and meteorological elements, the TMY-2 and TMY-3 data sets were created using procedures similar to those developed by Sandia National Laboratories (Hall et al., 1978). The format for the TMY-3 data however is radically different from that of the TMY and TMY-2. The older TMY formats used columnar or positional layouts to optimize the data storage space. Such formats though are difficult to read, and also it is difficult to import specific data fields into many software packages. Therefore the comma-separated value (CSV) format is adopted in TMY-3 which is ubiquitous, and many existing programs and applications provide built-in

functions to read or parse it. For compatibility with existing software, the National Renewable Energy Laboratory (NREL) has produced an application to convert from TMY-3 to TMY-2 format. Despite the format differences however, the fields in the TMY-3 are very similar to those in the TMY-2 data set. Fundamental differences are measurement units, which are SI or equivalent in the TMY-3, the addition of new fields for surface albedo and liquid precipitation, and the removal of the fields for present weather, snow depth, and days since last snowfall that were present in the TMY-2 (Wilcox and Marion, 2008). These fields were removed because of incompatible changes in the nature of the source data or because the source data were not available for many stations. The TMY-3 data format has two header lines and 8760 lines of data, each with 68 data fields. The header line 1 contains the same data as the ones shown in Table 2.7 with the difference that the "city" is replaced by the "station name", whereas header line 2 contains data field name and units. The field format of the rest of the lines is similar to the TMY-2 format shown in Table 2.8 except for the local standard time data fields at the beginning which are changed to "Date" in MM/DD/YYYY format and "Time" in HH:MM format and the other changes at the end of the data fields as noted above.

The volcanic eruptions of El Chichón in Mexico in March 1982 and Mount Pinatubo in the Philippines in June 1991 injected large amounts of aerosols into the stratosphere. The aerosols spread northward and circulated around the earth. This phenomenon noticeably decreased the amount of solar radiation reaching the earth during May 1982 until December 1984 due to El Chichón and from June 1991 to December 1994 due to Pinatubo, after which the effects of the aerosols diminished. Consequently, these months were not used in any of the TMY procedures because they were considered as non-typical (Wilcox and Marion, 2008). The TMY-3 data files for many US locations are available for download from the NREL web site (NREL, 2012).

Exercises

2.1 As an assignment using a spreadsheet program and the relations presented in this chapter, try to create a program that estimates all solar angles according to the latitude, day of year, hour, and slope of surface.

2.2 As an assignment using a spreadsheet program and the relations presented in this chapter, try to create a program that estimates all solar angles according to the latitude, day of year, and slope of surface for all hours of a day.

2.3 Calculate the solar declination for the spring and fall equinoxes and the summer and winter solstices.

2.4 Calculate the sunrise and sunset times and day length for the spring and fall equinoxes and the summer and winter solstices at 45°N latitude and 35°E longitude.

2.5 Determine the solar altitude and azimuth angles at 10:00 am local time for Rome, Italy, on June 10.

2.6 Calculate the solar zenith and azimuth angles, the sunrise and sunset times, and the day length for Cairo, Egypt, at 10:30 am solar time on April 10.

2.7 Calculate the sunrise and sunset times and altitude and azimuth angles for London, England, on March 15 and September 15 at 10:00 am and 3:30 pm solar times.

2.8 What is the solar time in Denver, Colorado, on June 10 at 10:00 am Mountain Standard Time?

2.9 A flat-plate collector in Nicosia, Cyprus, is tilted at 40° from horizontal and pointed 10° east of south. Calculate the solar incidence angle on the collector at 10:30 am and 2:30 pm solar times on March 10 and September 10.

2.10 A vertical surface in Athens, Greece, faces 15° west of due south. Calculate the solar incidence angle at 10:00 am and 3:00 pm solar times on January 15 and November 10.

2.11 By using the sun path diagram, find the solar altitude and azimuth angles for Athens, Greece, on January 20 at 10:00 am.

2.12 Two rows of 6 m wide by 2 m high flat-plate collector arrays tilted at 40° are facing due south. If these collectors are located in 35°N latitude, using the sun path diagram find the months of the year and the hours of day at which the front row will cast a shadow on the second row when the distance between the rows is 3 m. What should be the distance so there will be no shading?

2.13 Find the blackbody spectral emissive power at $\lambda = 8\ \mu m$ for a source at 400 K, 1000 K, and 6000 K.

2.14 Assuming that the sun is a blackbody at 5777 K, at what wavelength does the maximum monochromatic emissive power occur? What fraction of energy from this source is in the visible part of the spectrum in the range 0.38–0.78 μm?

2.15 What percentage of blackbody radiation for a source at 323 K is in the wavelength region 6–15 μm?

2.16 A 2-mm thick glass sheet has a refraction index of 1.526 and an extinction coefficient of $0.2\ cm^{-1}$. Calculate the reflectivity, transmissivity, and absorptivity of the glass sheet at 0°, 20°, 40°, and 60° incidence angles.

2.17 A flat-plate collector has an outer glass cover of 4 mm thick $K = 23\ m^{-1}$ and refractive index of 1.526, and a Tedlar inner cover with refractive index of 1.45. Calculate the reflectivity, transmissivity, and absorptivity of the glass sheet at a 40° incidence angle by considering Tedlar to be of a very small thickness; that is, absorption within the material can be neglected.

2.18 The glass plate of a solar greenhouse has a transmissivity of 0.90 for wavelengths between 0.32 and 2.8 μm and is completely opaque at shorter and longer wavelengths. If the sun is a blackbody radiating energy to the earth's surface at an effective temperature of 5770 K and the interior of the greenhouse is at 300 K, calculate the percent of incident solar radiation transmitted through the glass and the percent of thermal radiation emitted by the interior objects that is transmitted out.

2.19 A 30-m^2 flat-plate solar collector is absorbing radiation at a rate of $900\ W/m^2$. The environment temperature is 25 °C and the collector emissivity is 0.85. Neglecting conduction and convection losses, calculate the equilibrium temperature of the collector and the net radiation exchange with the surroundings.

2.20 Two large parallel plates are maintained at 500 K and 350 K, respectively. The hotter plate has an emissivity of 0.6 and the colder one 0.3. Calculate the net radiation heat transfer between the plates.

2.21 Find the direct normal and horizontal extraterrestrial radiation at 2:00 pm solar time on February 21 for 40°N latitude and the total solar radiation on an extraterrestrial horizontal surface for the day.

2.22 Estimate the average hourly diffuse and total solar radiation incident on a horizontal surface for Rome, Italy, on March 10 at 10:00 am and 1:00 pm solar times if the monthly average daily total radiation is $18.1\ MJ/m^2$.

2.23 Calculate the beam and total radiation tilt factors and the beam and total radiation incident on a surface equator 1 h after local solar noon on April 15. The surface is located at 40°N latitude and the ground reflectance is 0.25. For that day, the beam radiation at normal incidence is $G_B = 710$ W/m^2 and diffuse radiation on the horizontal is $G_D = 250$ W/m^2.

2.24 For a south-facing surface located at 45°N latitude and tilted at 30° from the horizontal, calculate the hourly values of the beam radiation tilt factor on September 10.

2.25 A collector located in Berlin, Germany is tilted at 50° and receives a monthly average daily total radiation $\overline{H}$ equal to 17 MJ/m^2 day. Determine the monthly mean beam and total radiation tilt factors for October for an area where the ground reflectance is 0.2. Also, estimate the monthly average daily total solar radiation on the surface.

References

ASHRAE, 1975. Procedure for Determining Heating and Cooling Loads for Computerizing Energy Calculations. ASHRAE, Atlanta.

ASHRAE, 2007. Handbook of HVAC Applications. ASHRAE, Atlanta.

Collares-Pereira, M., Rabl, A., 1979. The average distribution of solar radiation—correlations between diffuse and hemispherical and between daily and hourly insolation values. Sol. Energy 22 (2), 155–164.

Duffie, J.A., Beckman, W.A., 1991. Solar Engineering of Thermal Processes. John Wiley & Sons, New York.

Dunkle, R.V., 1954. Thermal radiation tables and application. ASME Trans. 76, 549.

Erbs, D.G., Klein, S.A., Duffie, J.A., 1982. Estimation of the diffuse radiation fraction four hourly, daily and monthly-average global radiation. Sol. Energy 28 (4), 293–302.

Filkenstein, J.M., Schafer, R.E., 1971. Improved goodness of fit tests. Biometrica 58, 641–645.

Garg, H.P., 1982. Treatise on Solar Energy. In: Fundamentals of Solar Energy Research, vol. 1. John Wiley & Sons, New York.

Hall, I.J., Prairie, R.R., Anderson, H.E., Boes, E.C., 1978. Generation of typical meteorological years for 26 SOLMET stations. In: Sandia Laboratories Report, SAND 78-1601. Albuquerque, NM.

Hay, J.E., Davies, J.A., 1980. Calculations of the solar radiation incident on an inclined surface. In: Proceedings of the First Canadian Solar Radiation Data Workshop, 59. Ministry of Supply and Services, Canada.

Hottel, H.C., Woertz, B.B., 1942. Evaluation of flat plate solar heat collector. ASME Trans. 64, 91.

Hsieh, J.S., 1986. Solar Energy Engineering. Prentice-Hall, Englewood Cliffs, NJ.

Kalogirou, S.A., 2003. Generation of typical meteorological year (TMY-2) for Nicosia, Cyprus. Renewable Energy 28 (15), 2317–2334.

Klein, S.A., Beckman, W.A., Duffie, J.A., 1976. A design procedure for solar heating systems. Sol. Energy 18, 113–127.

Klucher, T.M., 1979. Evaluation of models to predict insolation on tilted surfaces. Sol. Energy 23 (2), 111–114.

Kreith, F., Kreider, J.F., 1978. Principles of Solar Engineering. McGraw-Hill, New York.

Liu, B.Y.H., Jordan, R.C., 1960. The interrelationship and characteristic distribution of direct, diffuse and total solar radiation. Sol. Energy 4 (3), 1–19.

Liu, B.Y.H., Jordan, R.C., 1977. Availability of solar energy for flat plate solar heat collectors. In: Liu, B.Y.H., Jordan, R.C. (Eds.), Application of Solar Energy for Heating and Cooling of Buildings. ASHRAE, Atlanta.

Löf, G.O.G., Tybout, R.A., 1972. Model for optimizing solar heating design. ASME paper, 72-WA/SOL-8.

Marion, W., Urban, K., 1995. User's Manual for TMY2s Typical Meteorological Years. National Renewable Energy Laboratory, Colorado.

Meinel, A.B., Meinel, M.P., 1976. Applied Solar Energy—An Introduction. Addison-Wesley, Reading, MA.

Meteonorm, 2009. Maps. Available from: www.meteonorm.com.
NREL, 2012. TMY-3 Data Files. Available from: http://rredc.nrel.gov/solar/old_data/nsrdb/1991-2005/tmy3.
Page, J.K., 1964. The estimation of monthly mean values of daily total short-wave radiation of vertical and inclined surfaces from sunshine records for latitudes 40°N-40°S. Proc. UN Conf. New Sources Energy 4, 378.
Reindl, D.T., Beckman, W.A., Duffie, J.A., 1990. Diffuse fraction correlations. Sol. Energy 45 (1), 1–7.
Reindl, D.T., Beckman, W.A., Duffie, J.A., 1990. Evaluation of hourly tilted surface radiation models. Sol. Energy 45 (1), 9–17.
Siegel, R., Howell, J.R., 2002. Thermal Radiation Heat Transfer, fourth ed. Taylor and Francis, New York.
Solar Spectra, 2007. Air Mass Zero. Available from: http://rredc.nrel.gov/solar/spectra/am0.
Spencer, J.W., 1971. Fourier series representation of the position of the sun. Search 2 (5), 172.
Wilcox, S., Marion, W., 2008. Users Manual for TMY3 Data Sets Technical Report NREL/TP-581-43156 (Revised May 2008).